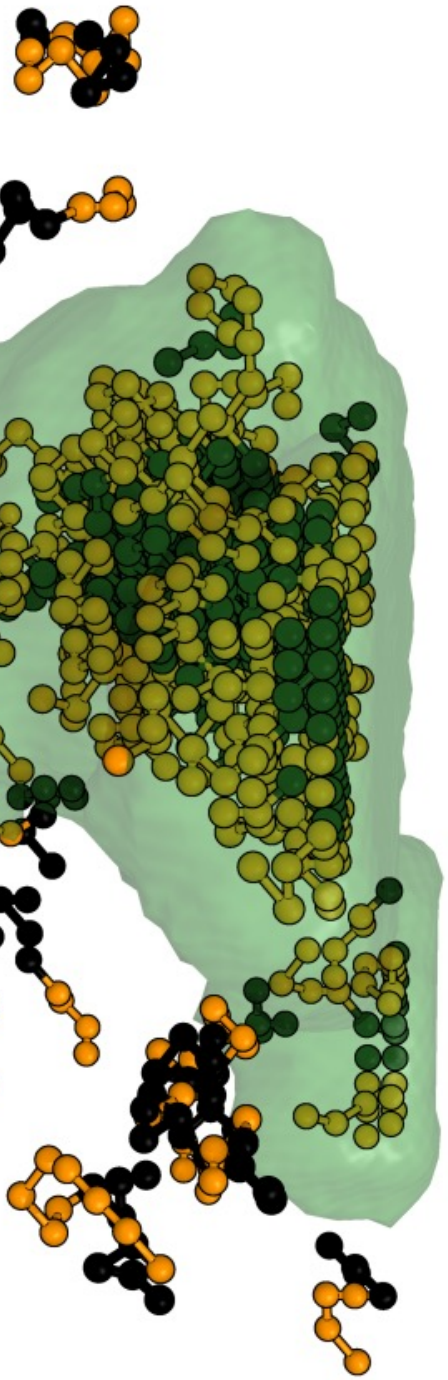

Molecular Simulation of Soft Matter Self-Assembly and Phase Behavior

Andrew Santos, PhD

TSM Branch Seminar

October, 13th 2021

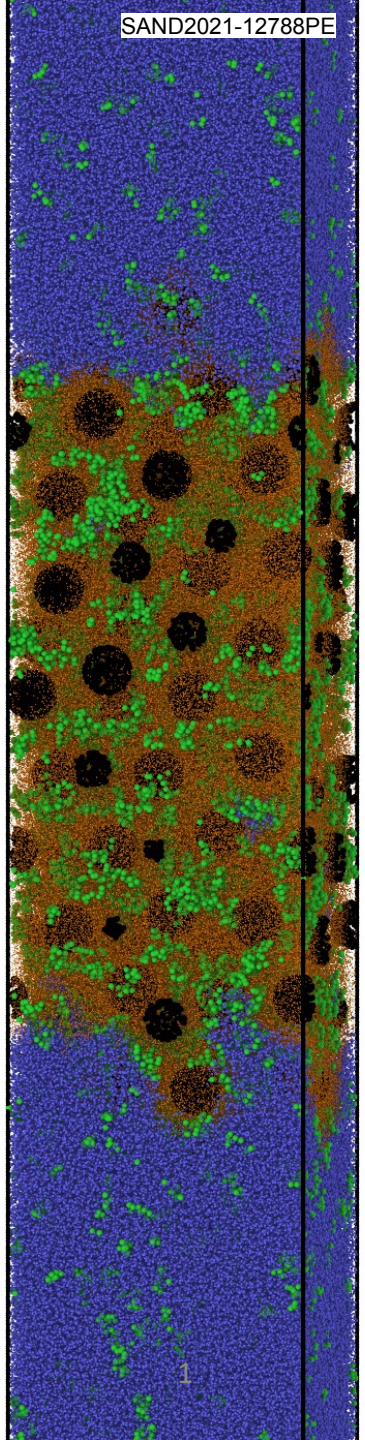

SAND2021-12788PE

Materials

Surfactants

nonionic

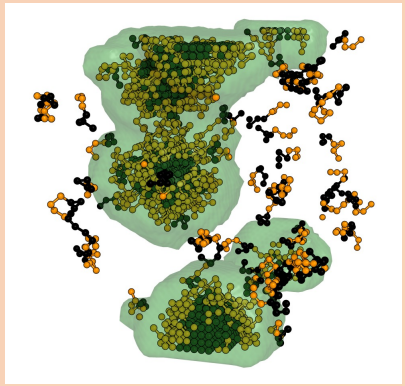

ionic

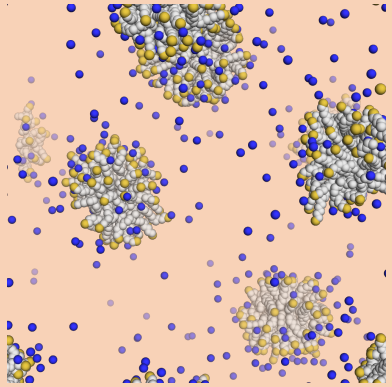

SALR Colloids

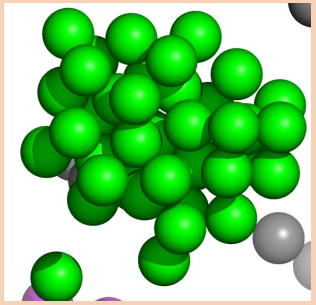

Nanocomposites

Grafted-NP

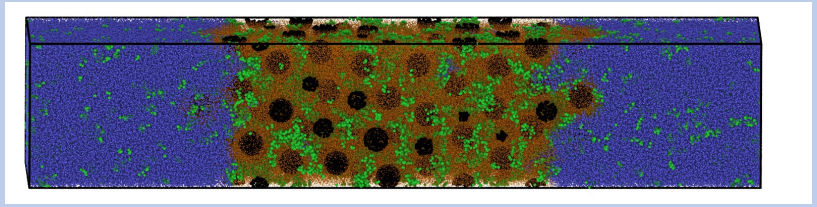

Magnetic

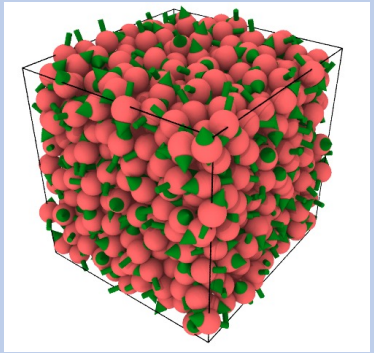

Bare NPs

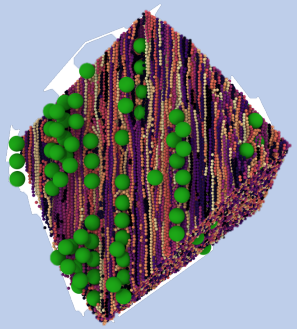

Granular

Packings

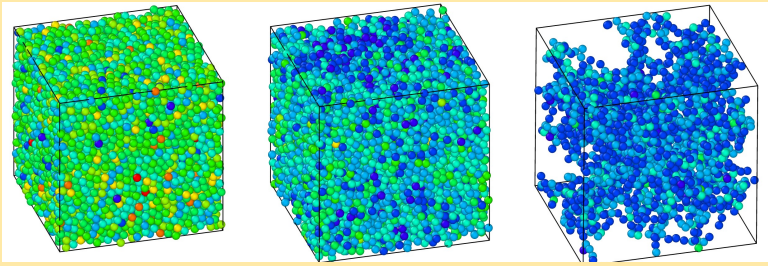

Flow

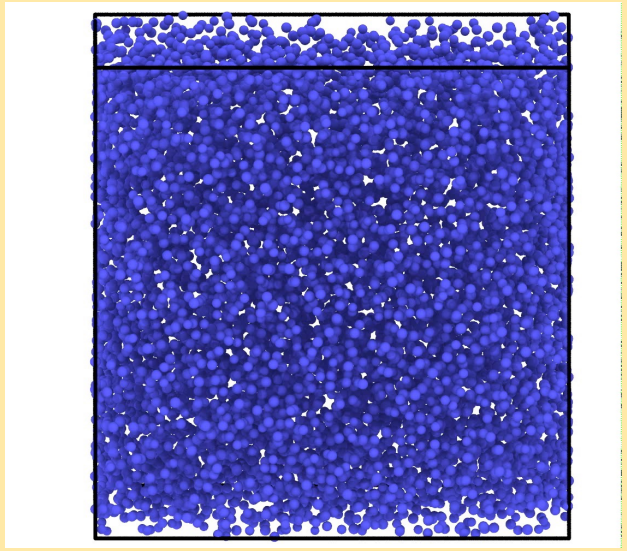

Methods

Surfactants

Molecular Dynamics (MD)
- *NVT* ensembles
- Gromacs, Hoomd, LAMMPS

Monte Carlo (MC)
- *μVT, NVT* ensembles
- Cassandra, Legacy code (Fortran)

Law-of-mass-action modelling

Nanocomposites

Molecular dynamics
Theoretically-informed Langevin dynamics (TILD)
- MD evolves simulation of particles
- Force on particle is calculated from a field-based interaction
- Fast for dense systems
- Thermal fluctuations
- Implemented into LAMMPS

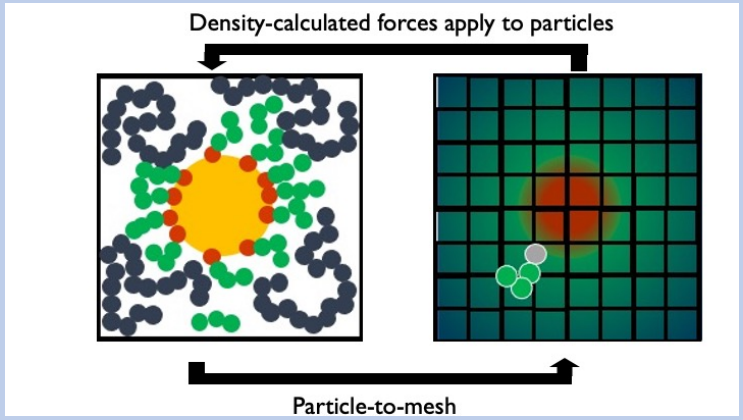

Granular

Discrete element modeling (DEM)
- Forces calculated at contact
- Requires memory of interaction
- Dissipative, out-of-equilibrium
- LAMMPS

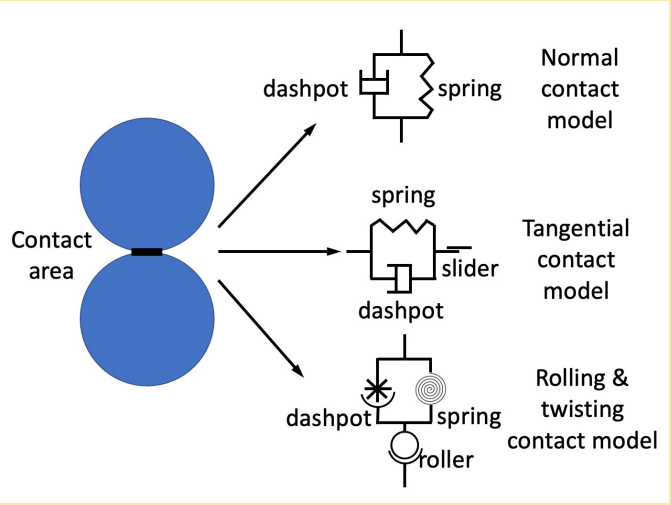

Materials

Surfactants

nonionic

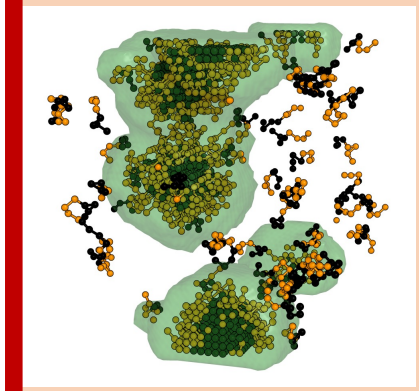

ionic

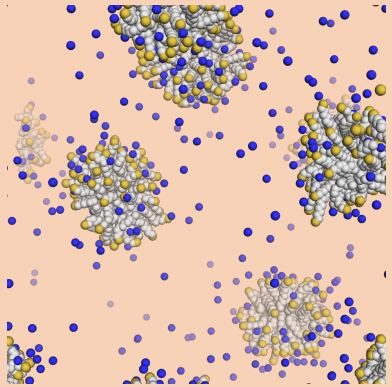

Colloids

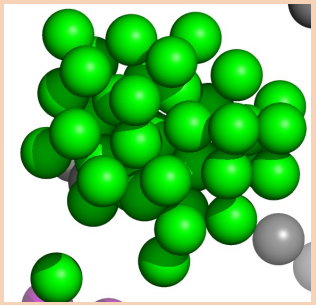

Nanocomposites

Grafted-NP

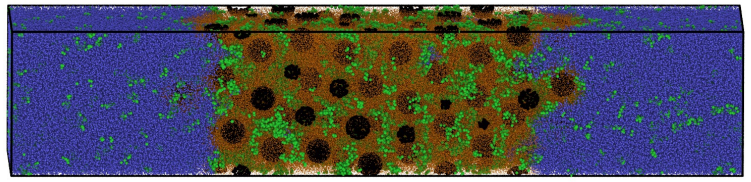

Magnetic

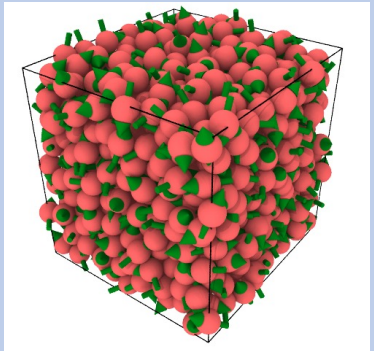

Bare NPs

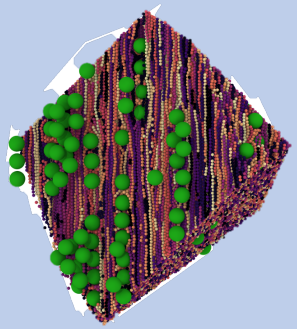

Granular

Packings

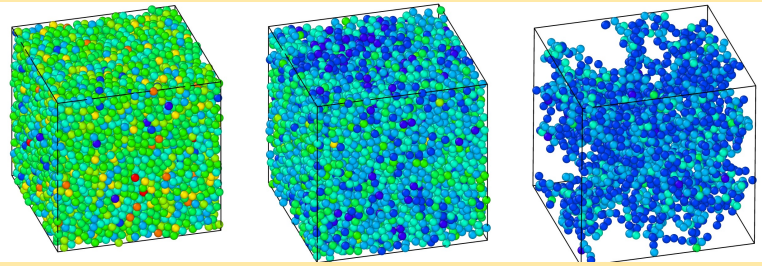

Flow

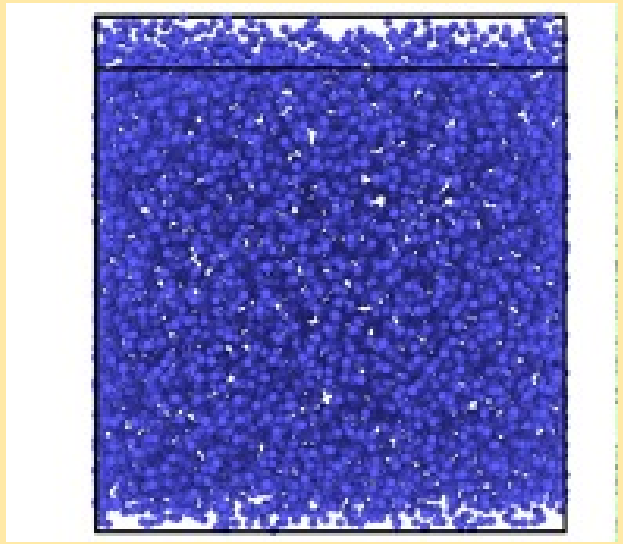

Amphiphile self-assembly for complex materials

Detergency

Thin films

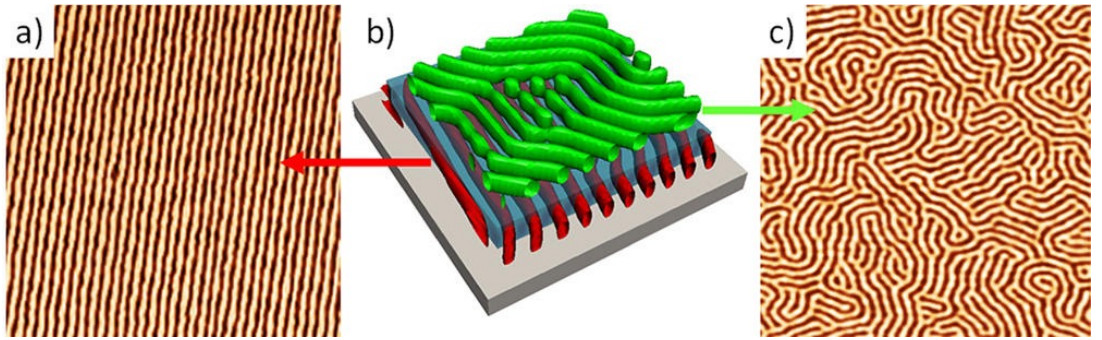

Register et al., *Macromolecules*, 7588–7596, 2016

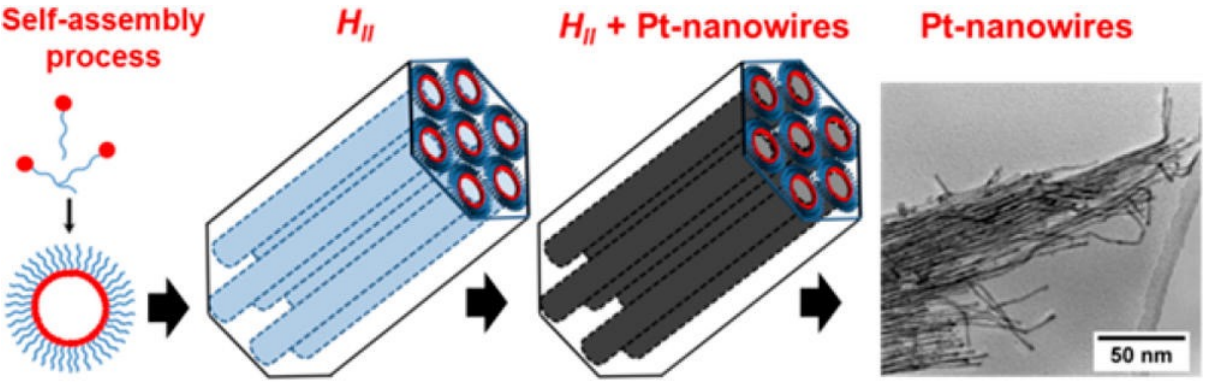

Nanotechnology

Squires et al., *Langmuir*, 6991−6996, 2018

Biology

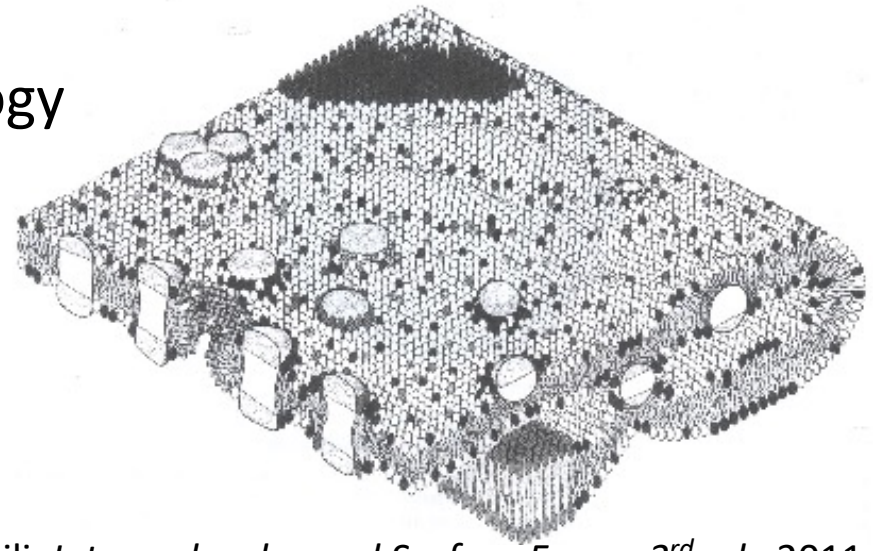

Israelachvili, *Intermolecular and Surface Forces 3rd ed.*, 2011

Surfactant micellization

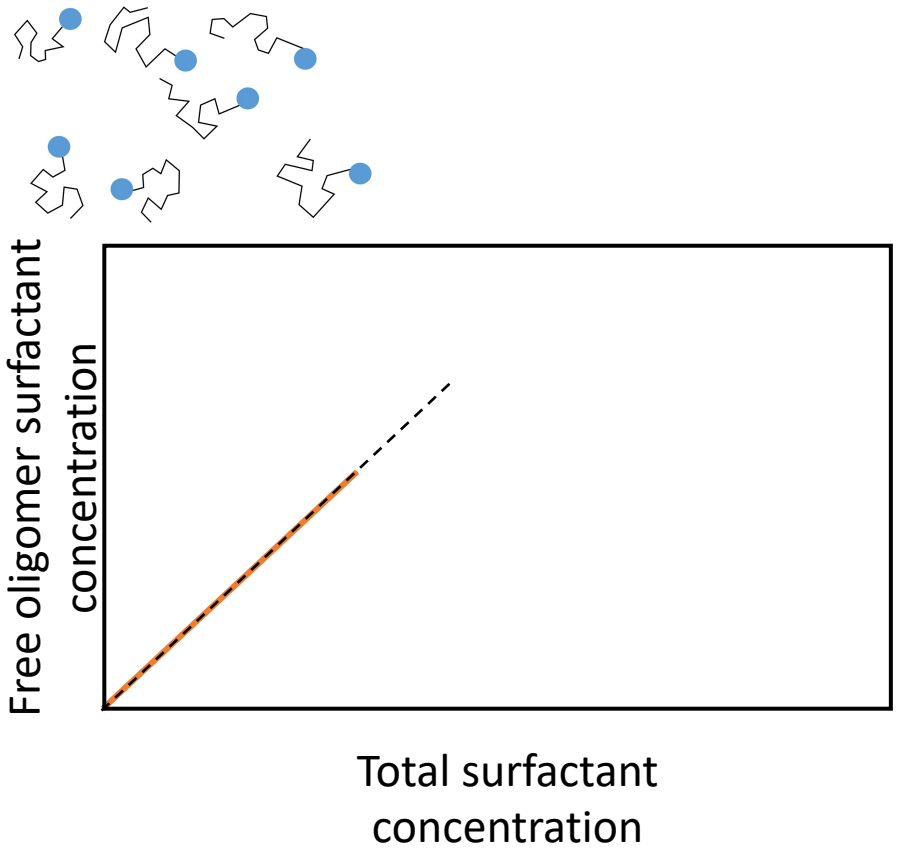

Surfactant micellization

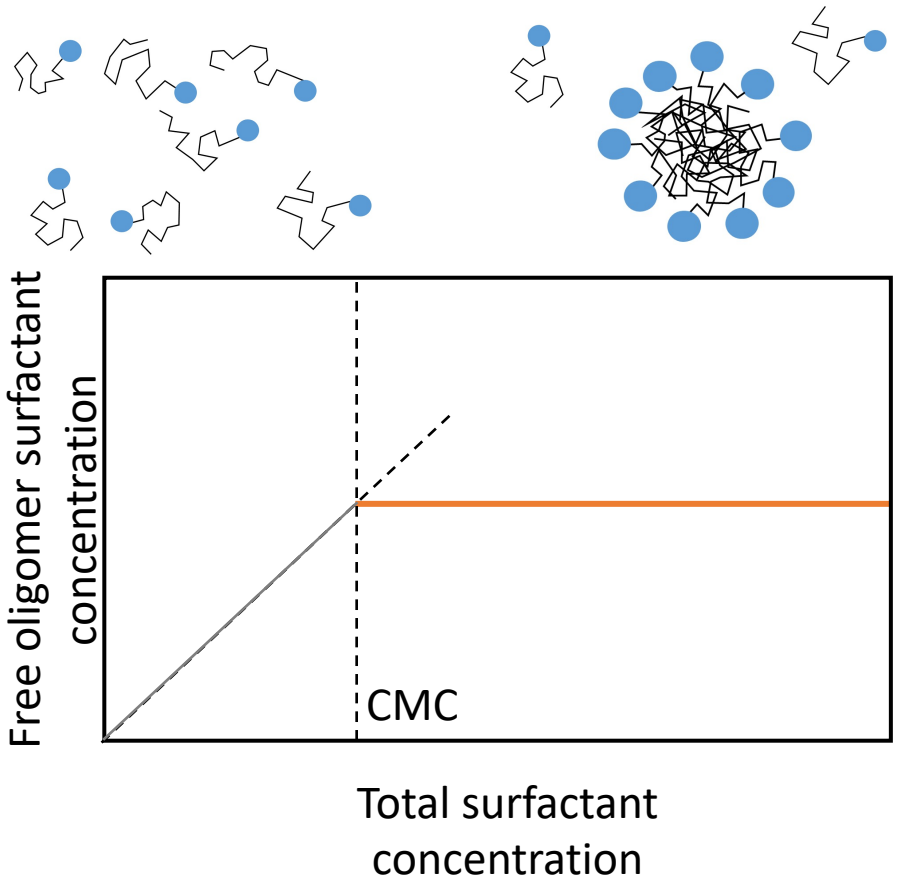

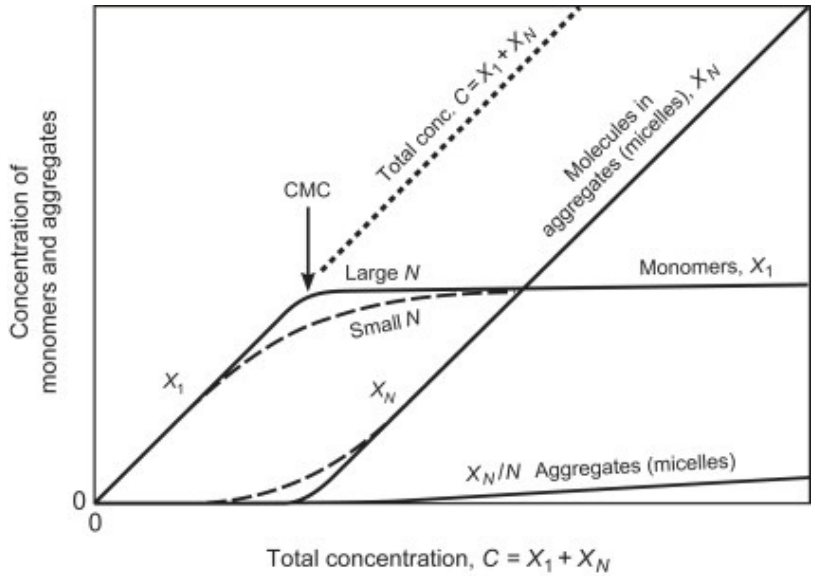

Israelachvili, *Intermolecular and Surface Forces* 3rd *ed.*, 2011

Surfactant micellization

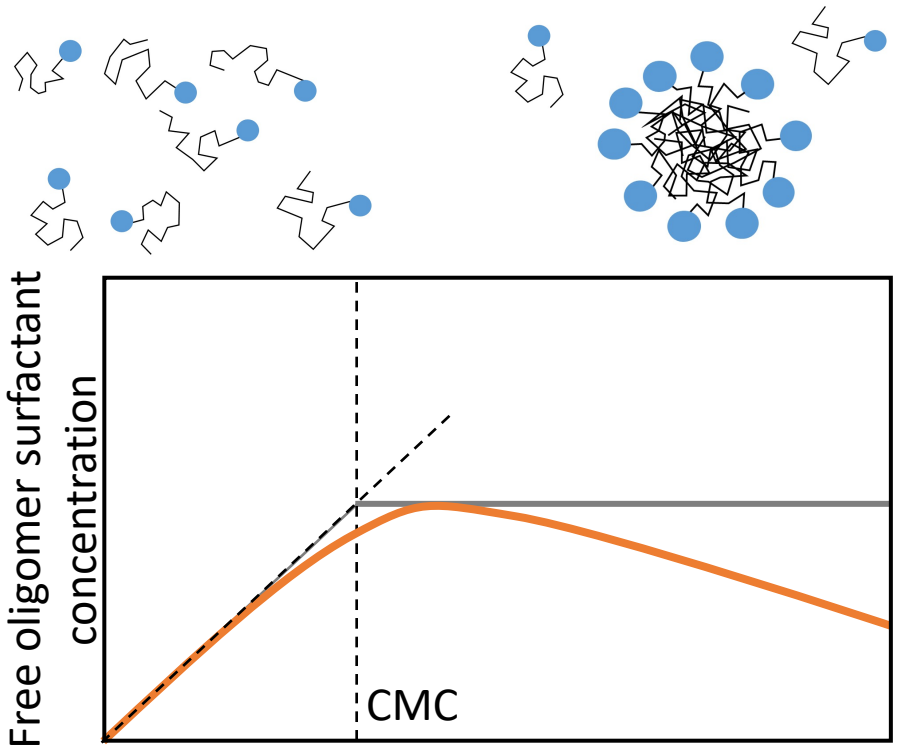

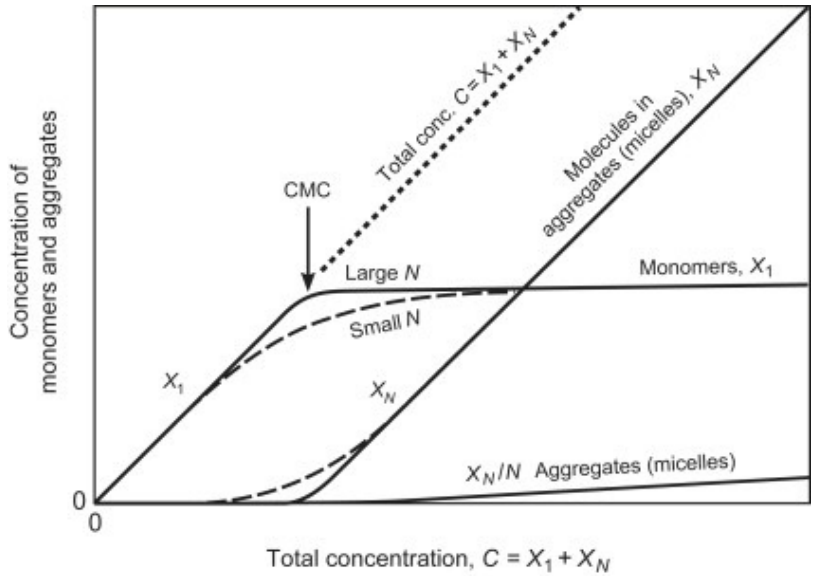

Israelachvili, *Intermolecular and Surface Forces* 3rd *ed.*, 2011

Surfactant micellization

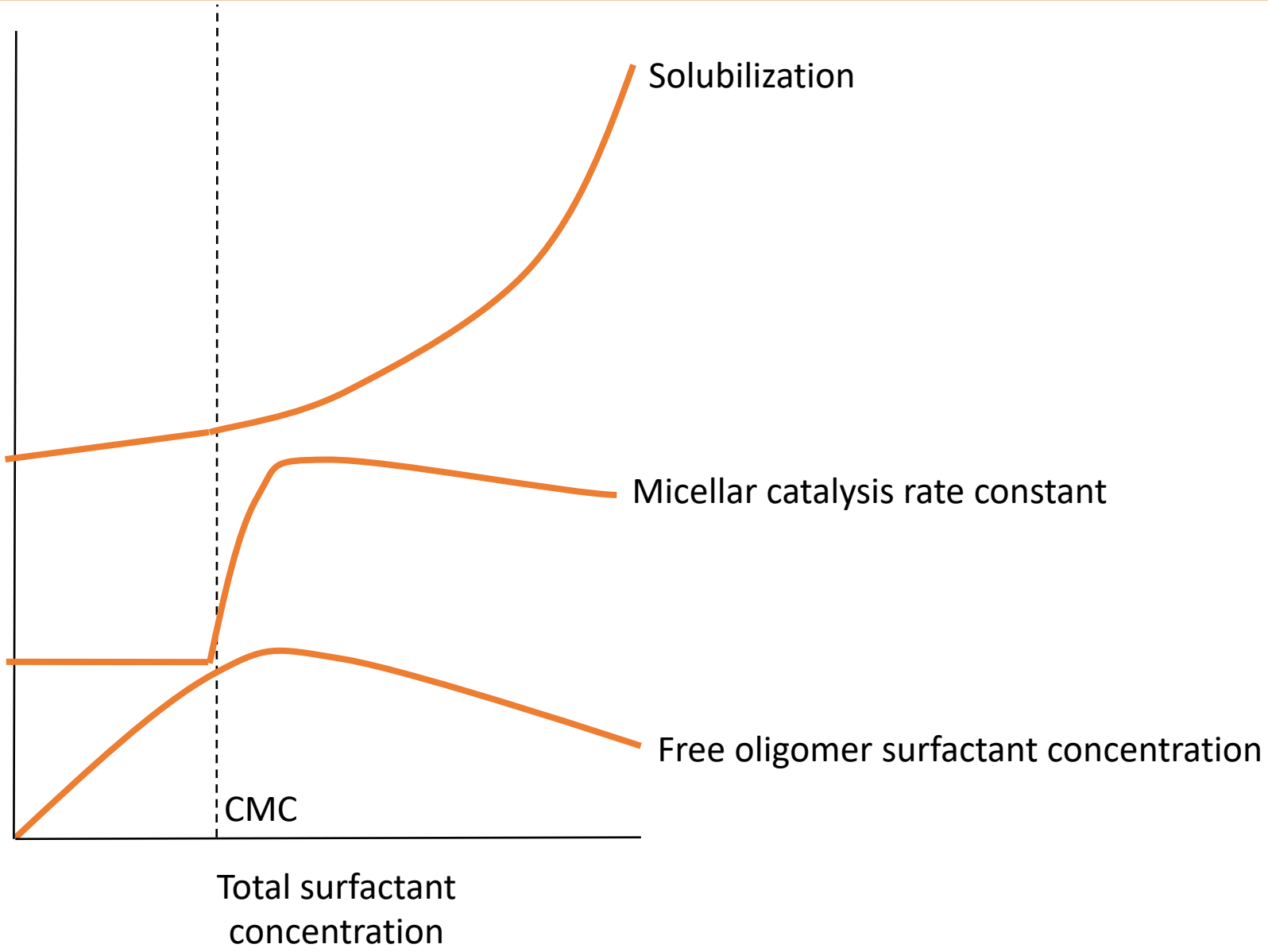

Surfactant micellization

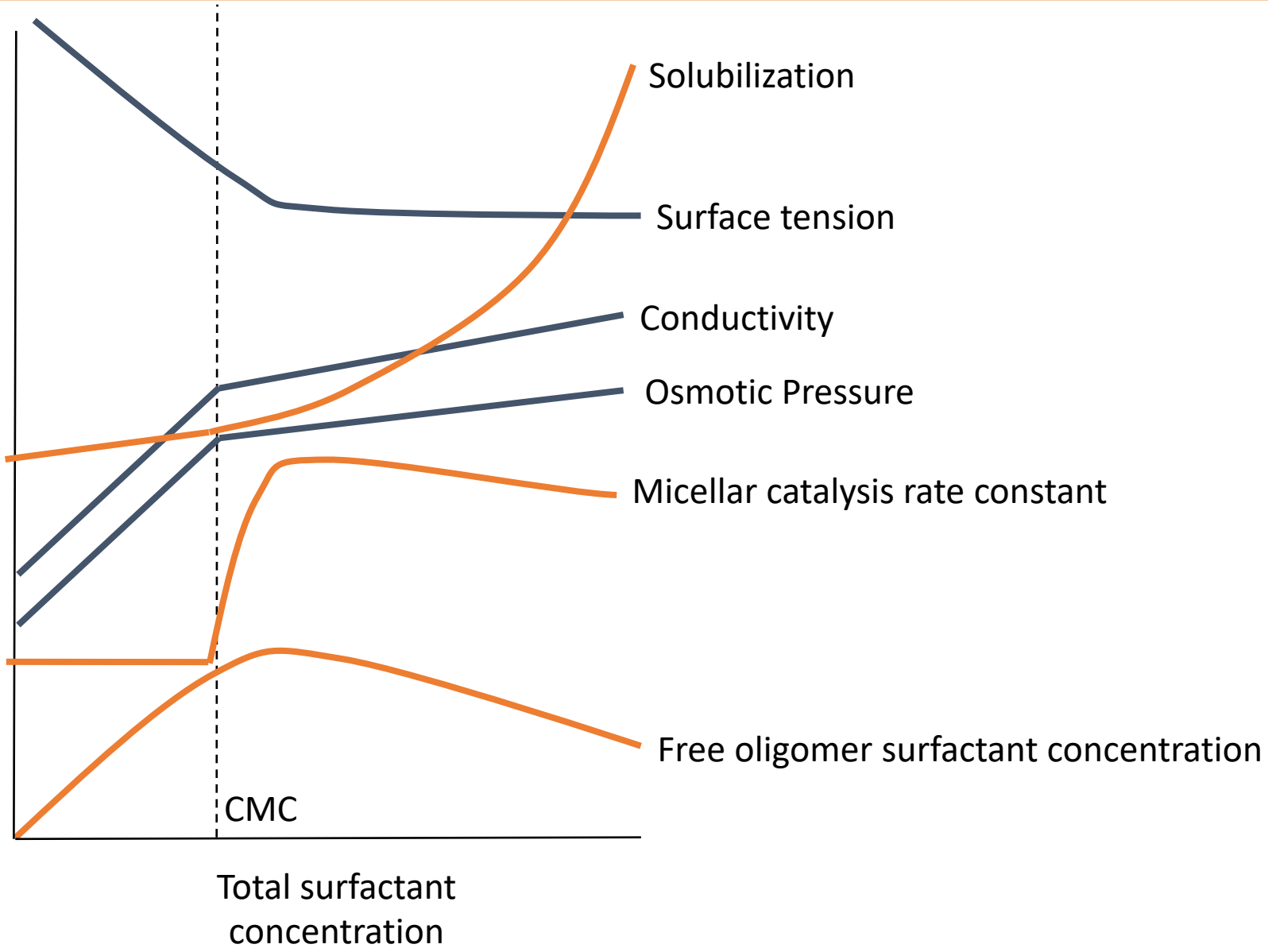

Importance of free surfactant effects

Tear-free shampoo

Johnsonsbaby.com, Cetaphil.com, loreal.com

Nanoparticle dispersion

Hsieh et al, *J. Phys. Chem. B*, 7950-8, 2013

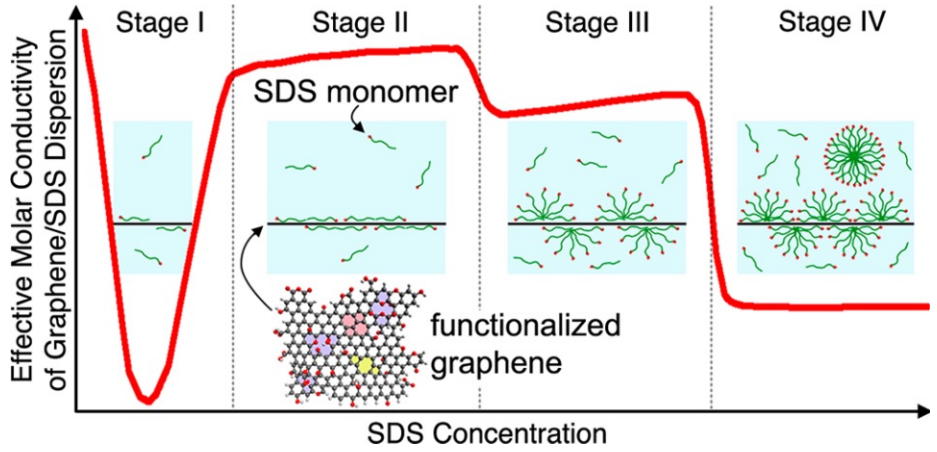

Experimental Measurement

Property	Technique
α, ΔG°	Specific conductivity
$\langle M \rangle$	Nuclear magnetic resonance
α, $\langle M \rangle$	Fluorescence quenching
$\langle M \rangle$	Light Scattering

Critical micelle Simulation measurement

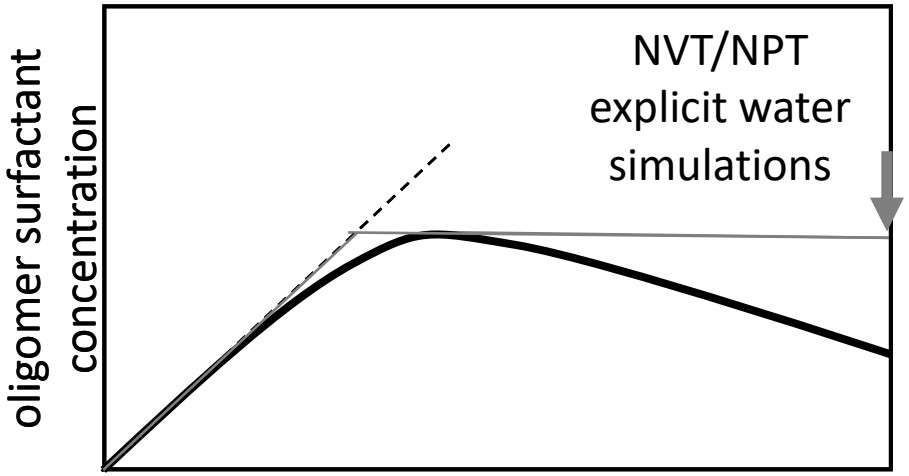

Monte Carlo Simulation Methods

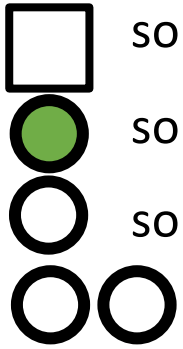

solvent

solvophilic (H)

solvophobic (T)

$\varepsilon_{TT} = -2$

$\varepsilon_{TH} = 0 = \varepsilon_{HH}$

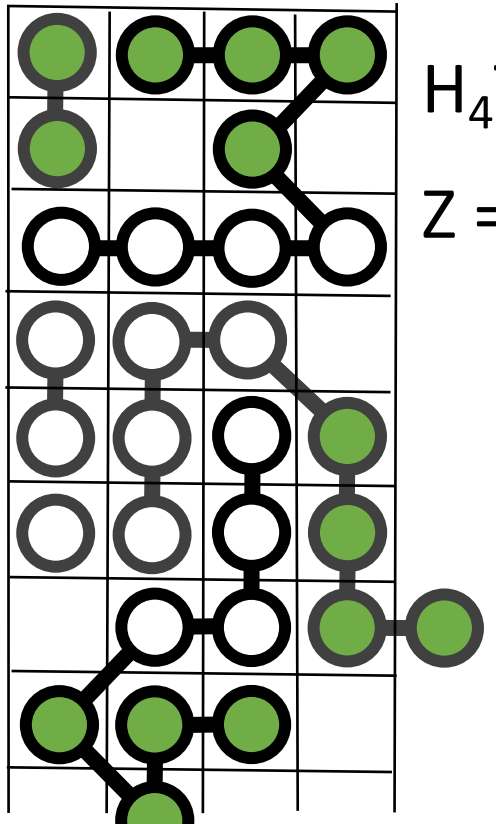

H_4T_4

$Z = 26$

Monte Carlo

- Grand-canonical (μVT) and canonical (NVT) ensembles
- Histogram reweighting

Ensemble \ Move	Reptations	Insertion/ deletions	Cluster moves
NVT	99.5%	0%	0.5%
μVT	39.5%	60%	0.5%

Larson et al., *J. Chem. Phys.*, 83, 1985

Free surfactant concentration

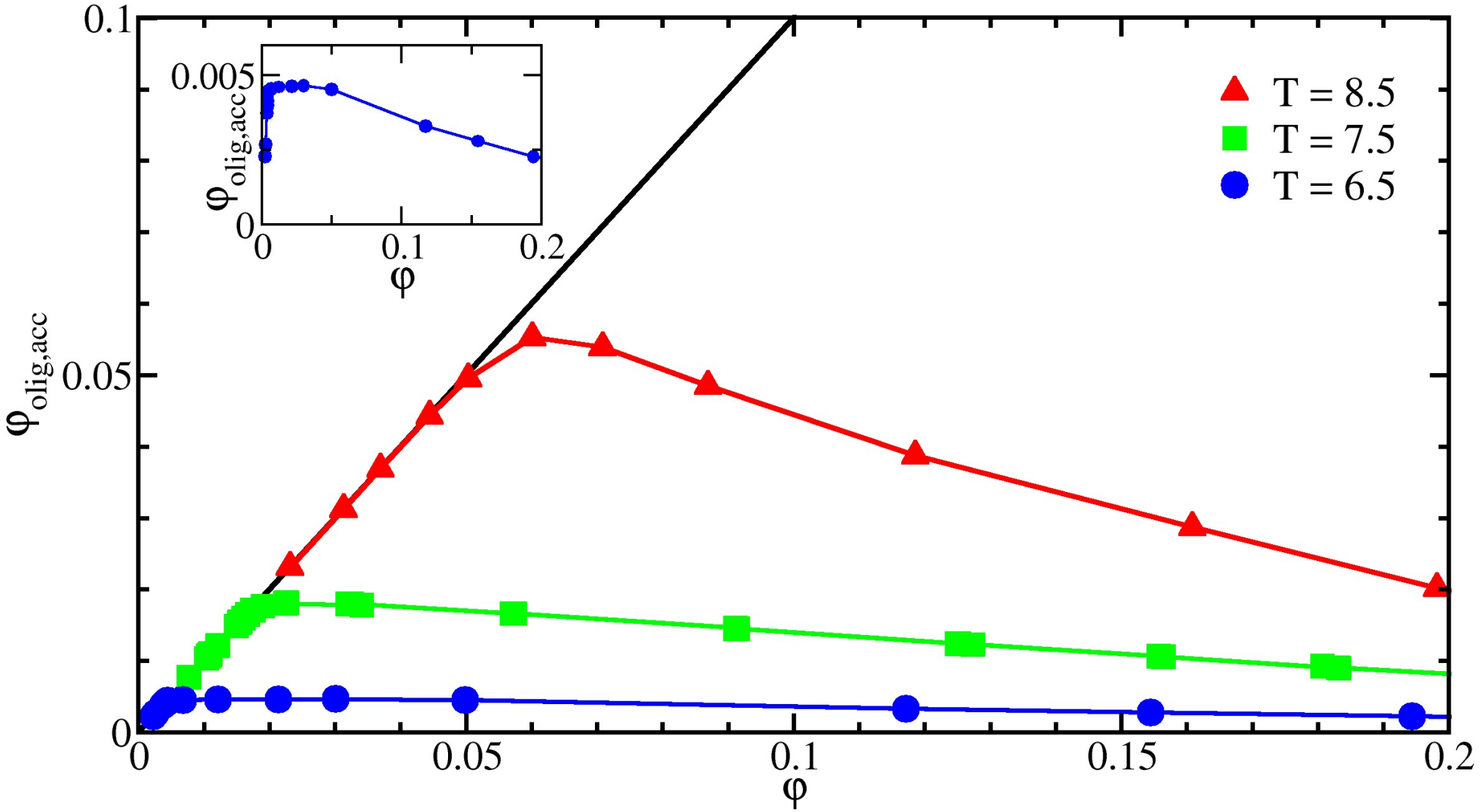

A. Santos & A. Panagiotopoulos, *J. Chem. Phys.*, 144 (4), 2016

Free volume

Free volume calculation method

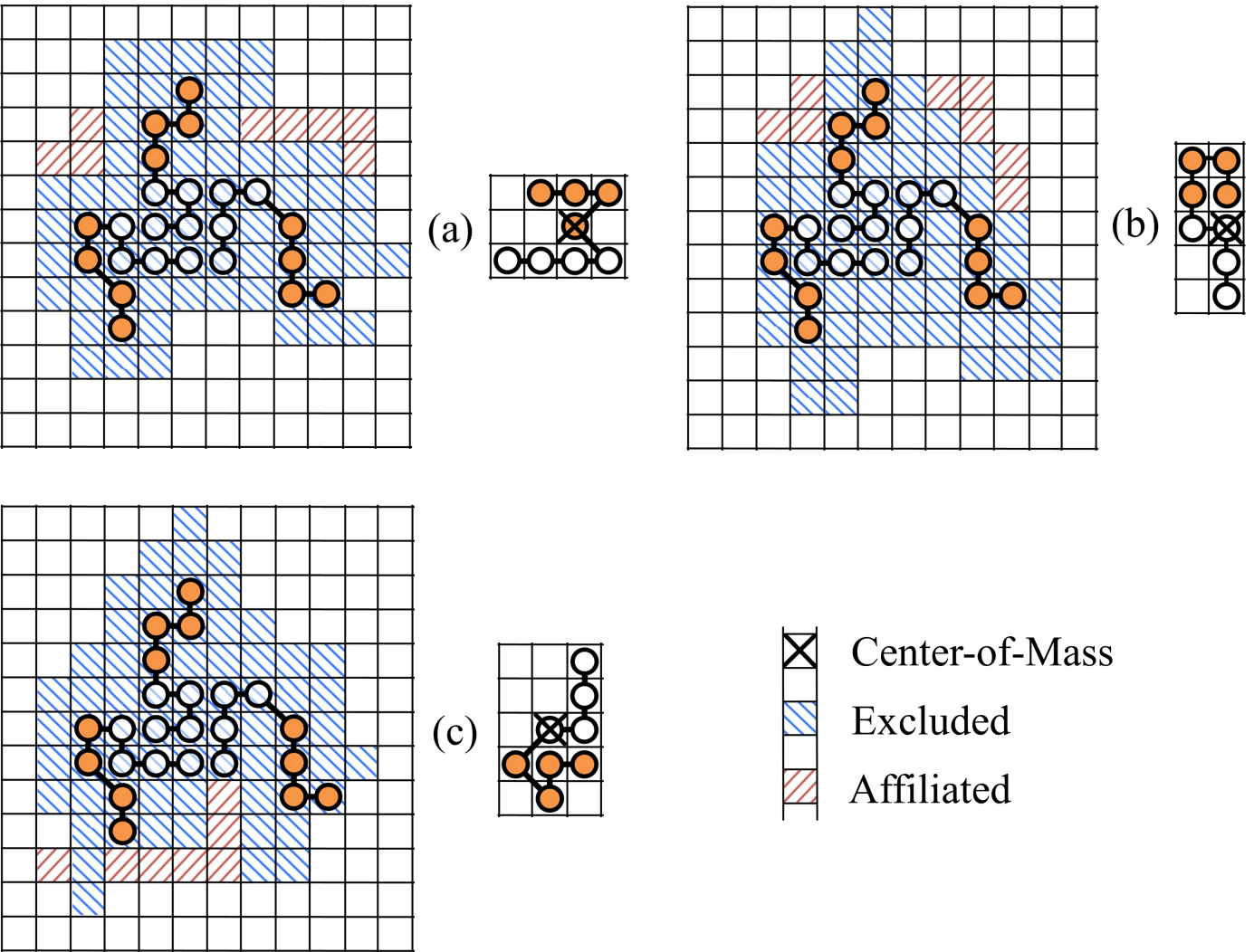

Free volume of a typical micellar system

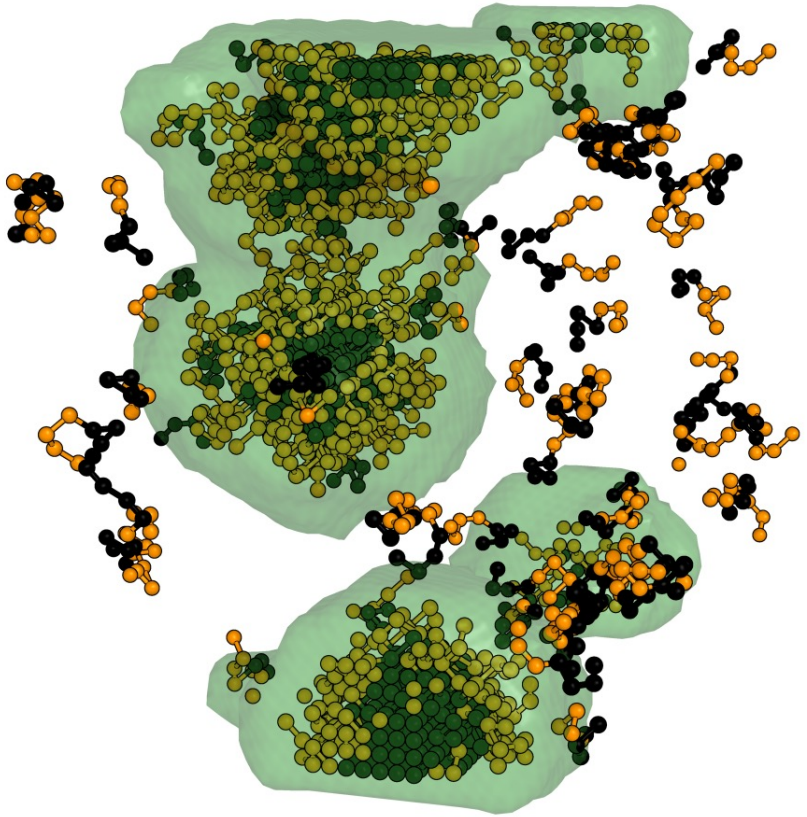

A. Santos & A. Panagiotopoulos, *J. Chem. Phys.*, 144 (4), 2016

Correcting the nonionic free surfactant volume fraction

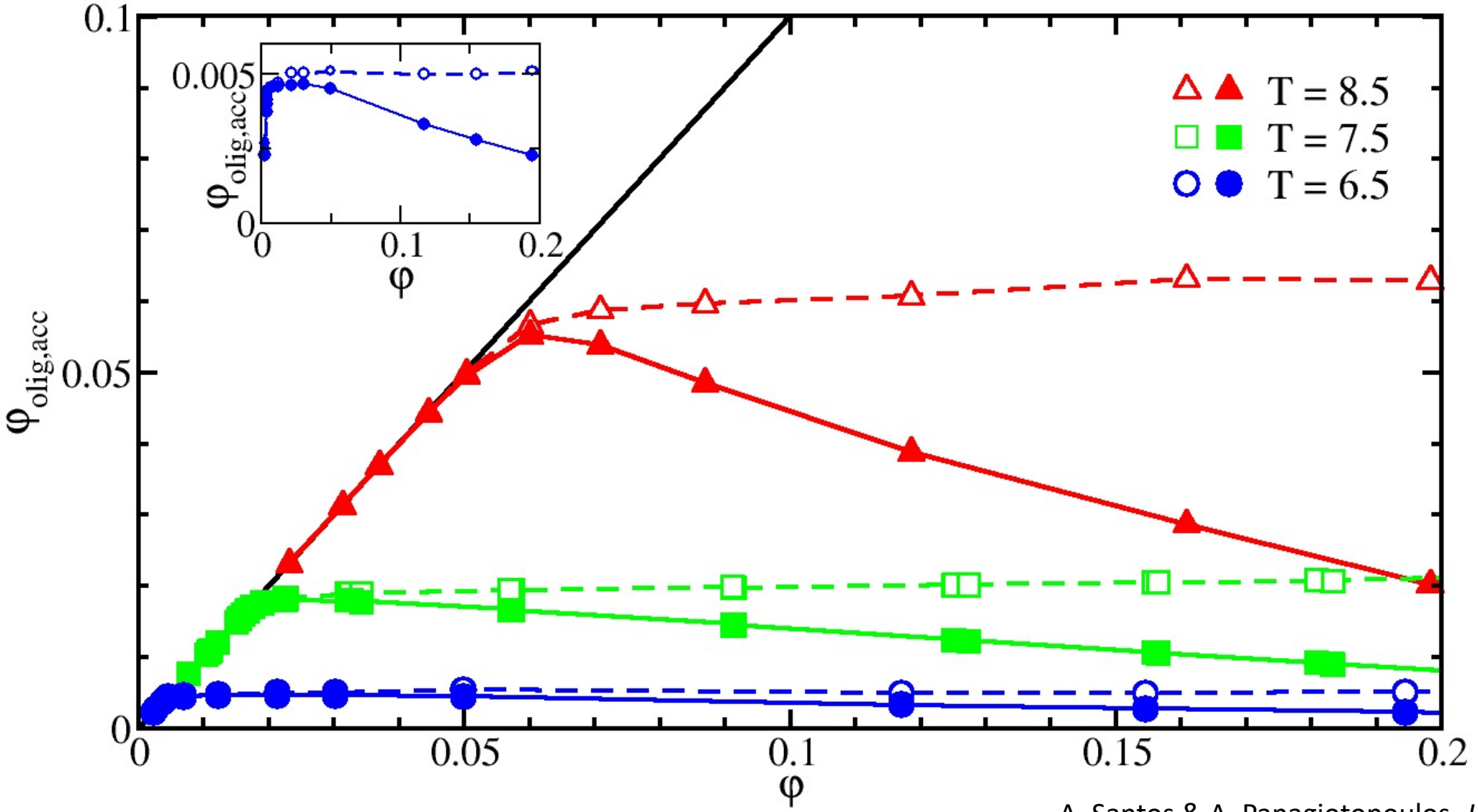

A. Santos & A. Panagiotopoulos, *J. Chem. Phys.*, 144 (4), 2016

Summary – Nonionic surfactants

- The decrease in the free amphiphile oligomer volume fraction is an equilibrium phenomena.
- The inaccessible volume successfully accounts for decrease in the volume fraction.
- Similar results were found for other surfactant architectures:

  S. Jiao, A. Santos & A. Panagiotopoulos, *Fluid Phase Equilibria*, 470, 2018

Experimental evidence

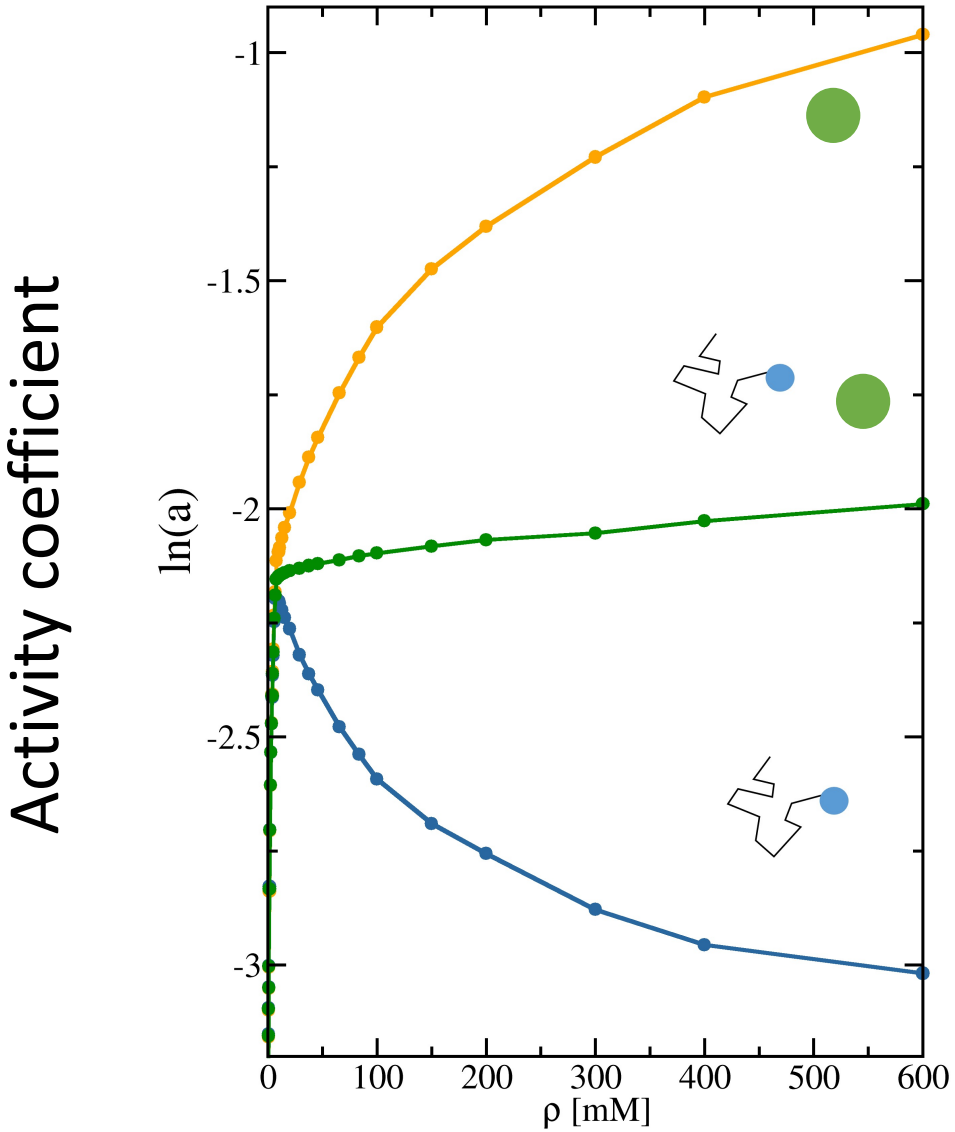

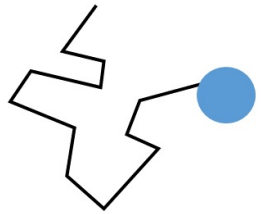

Ionic surfactant

counterion

Phenomena:

- Free volume
- "Salting-in" via the degree-of-association (α)

Evans et al., J. *Phys. Chem.*, 84, 1980

Experimental evidence

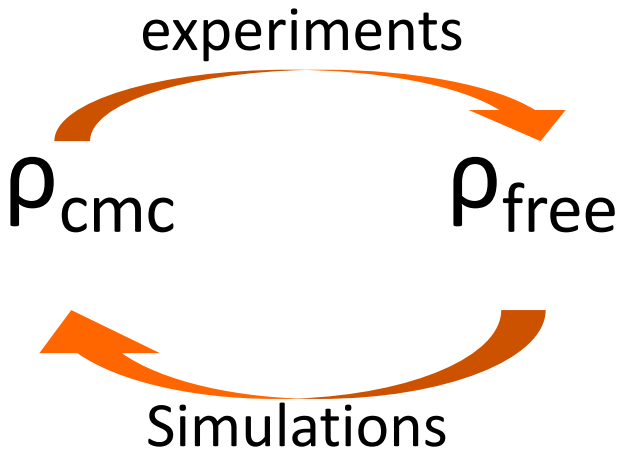

$$\rho_{\text{cmc}} = \exp\left[\frac{1}{(1+\alpha)}\left(\ln \rho_{\text{free}} + \alpha \ln\left(\frac{(1-\alpha)(\rho-\rho_{\text{free}})+\rho_{\text{free}}}{V_{\text{accessible}}}\right)\right)\right]$$

Bales, *J. Phys. Chem. B,* 105, 2001
Quina *et al.*, *J. Phys. Chem.*, 99, 1995
} experimental

Gunnarsson *et al.*, *J. Phys. Chem.*, 84, 1980
Jusufi *et al.*, *J. Phys. Chem. B,* 116, 2012
} theory

LeBard *et al.*, *Soft Matter,* 8, 2012
Sanders *et al.*, *J. Phys. Chem. B,* 116, 2012
} simulations

Simulation model

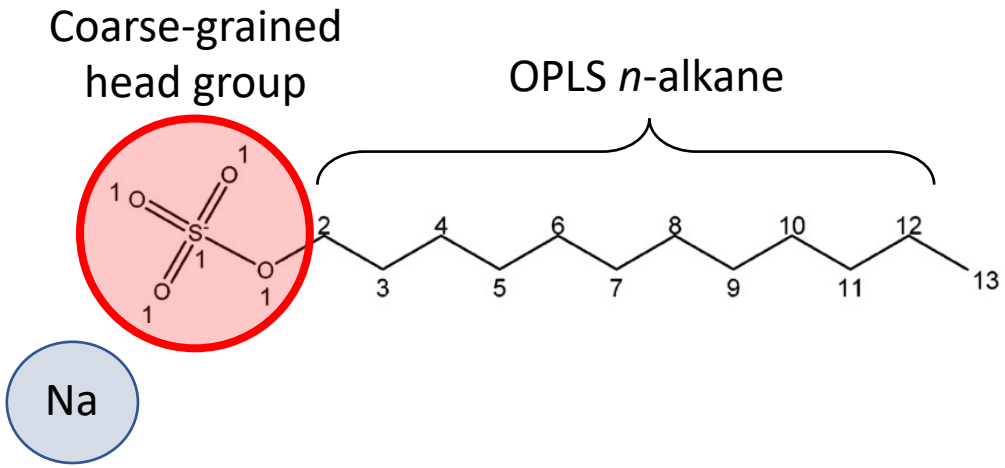

Sodium Dodecyl Sulfate

- Off-lattice, 3D
- Implicit-solvent (no water)

NVT MD simulations

	cmc [mM]		*M*	
surfactant	sim.	exp.	sim.	exp.
LiDS	9.1	8.7,[b] 8.9[c]	49	50,[c] 54[e]
NaDS	9.3	7.7,[f] 8.2,[b] 8.3,[c] 9.3[g]	57	50,[h] 53,[e] 64[i]
KDS	10	6.7,[g] 7.2[c]	55	60[c]
DTAB	16.4	14.6,[i] 14.9[j]	35	49,[i] 55[j]
DTAC	22.2	17.2,[k] 20.3,[j] 21.3[l]	31	45[j]

A. Jusufi, A. Hynninen and A. Z. Panagiotopoulos,
J. Phys. Chem. B, 112, 2008

Free surfactant concentration

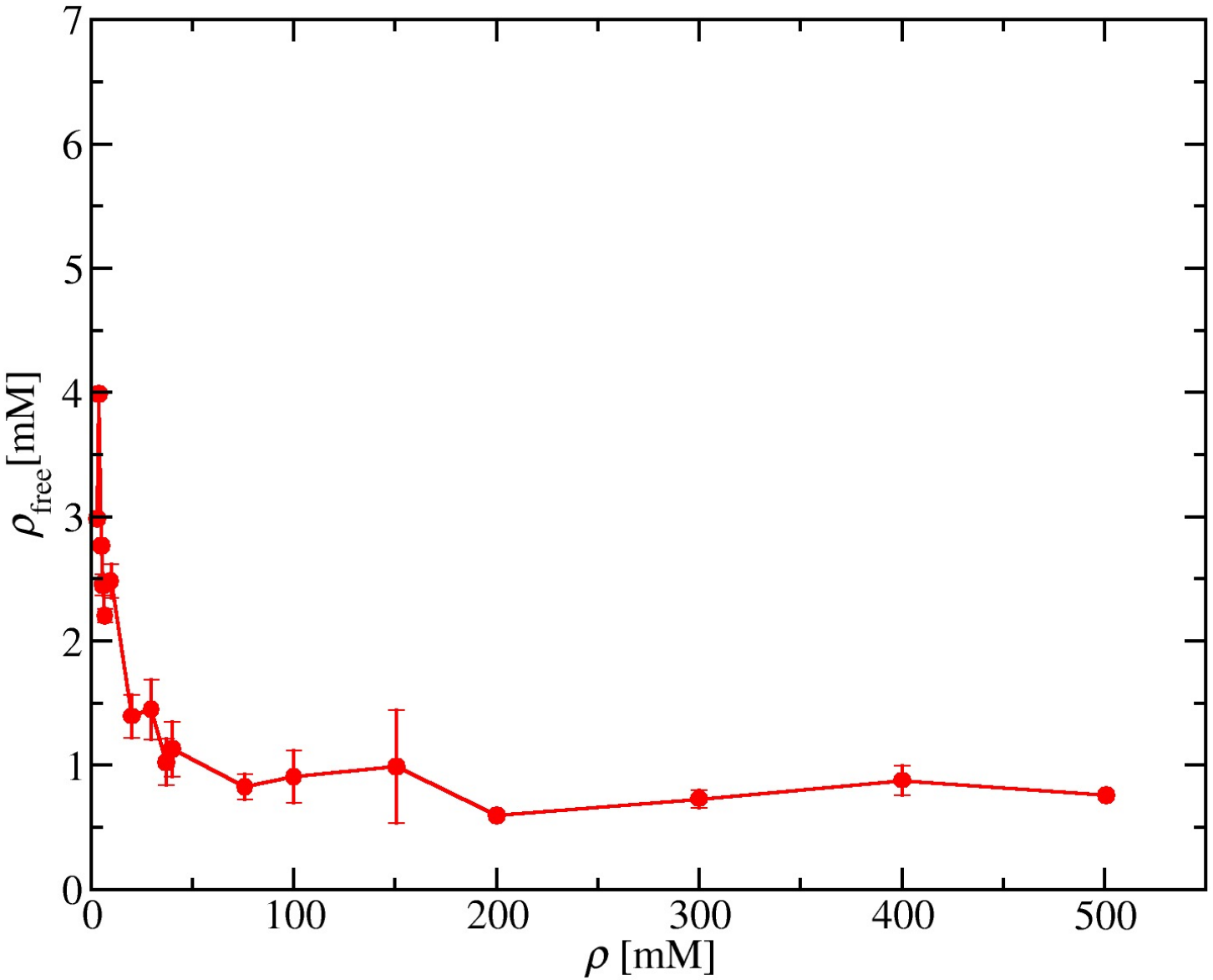

Excluded volume

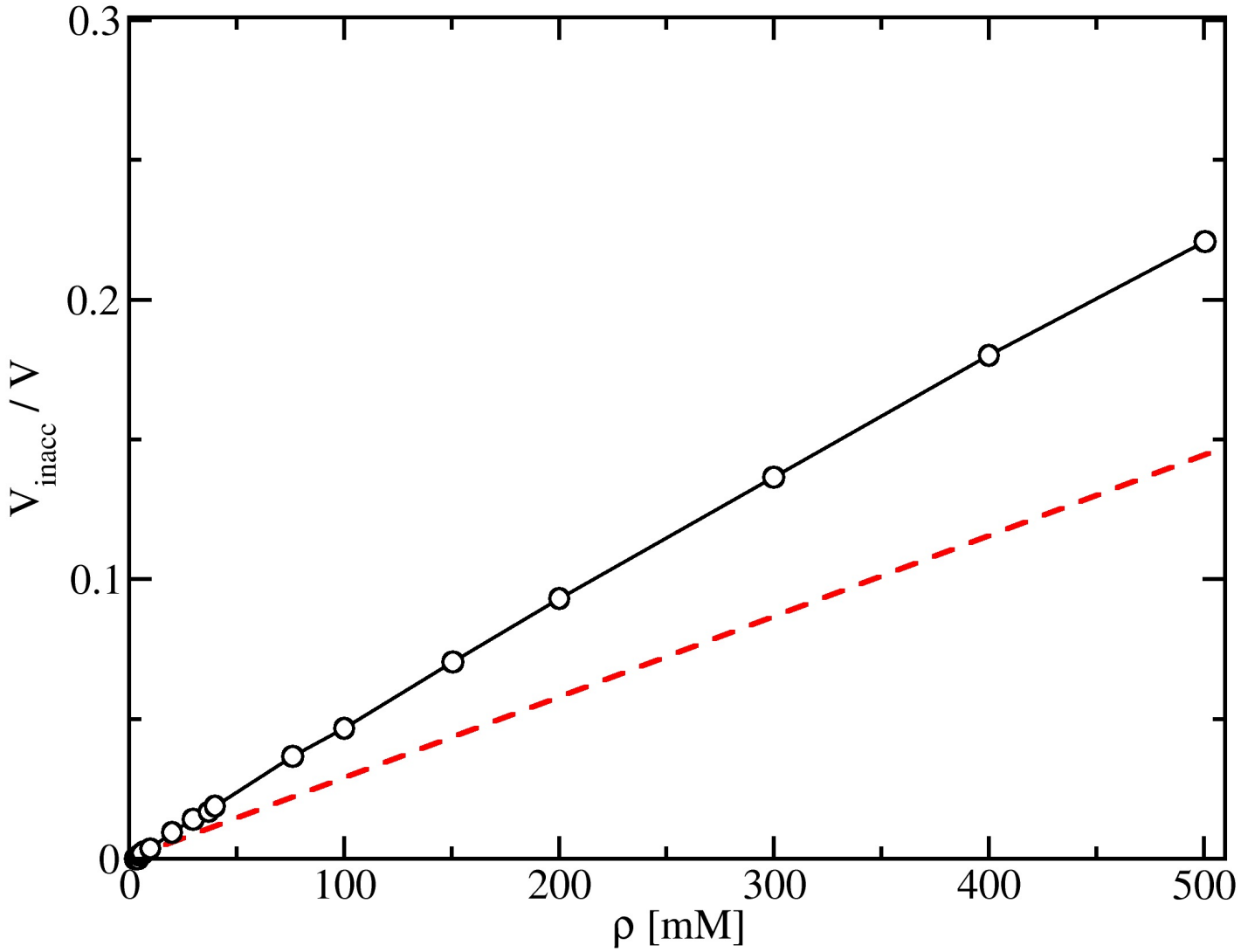

Excluded volume correction

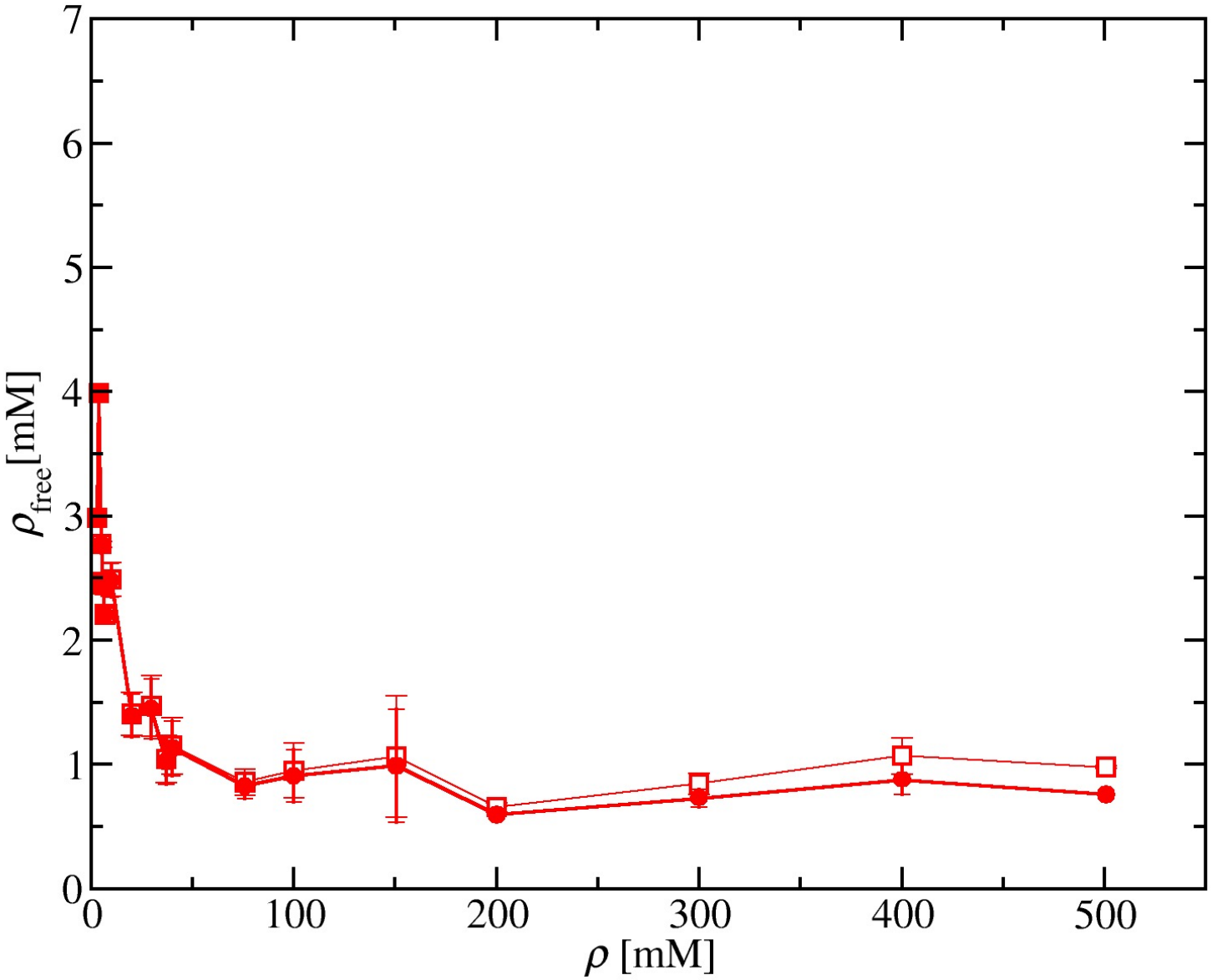

Degree of counterion association

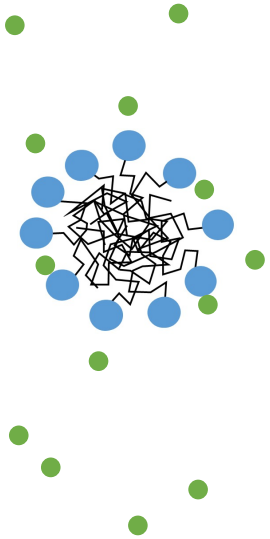

Degree of counterion association

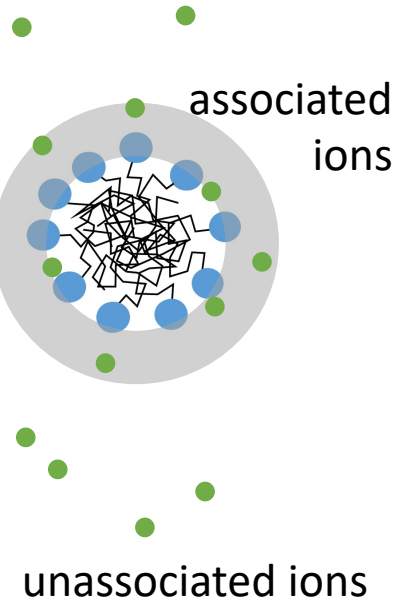

Degree of counterion association

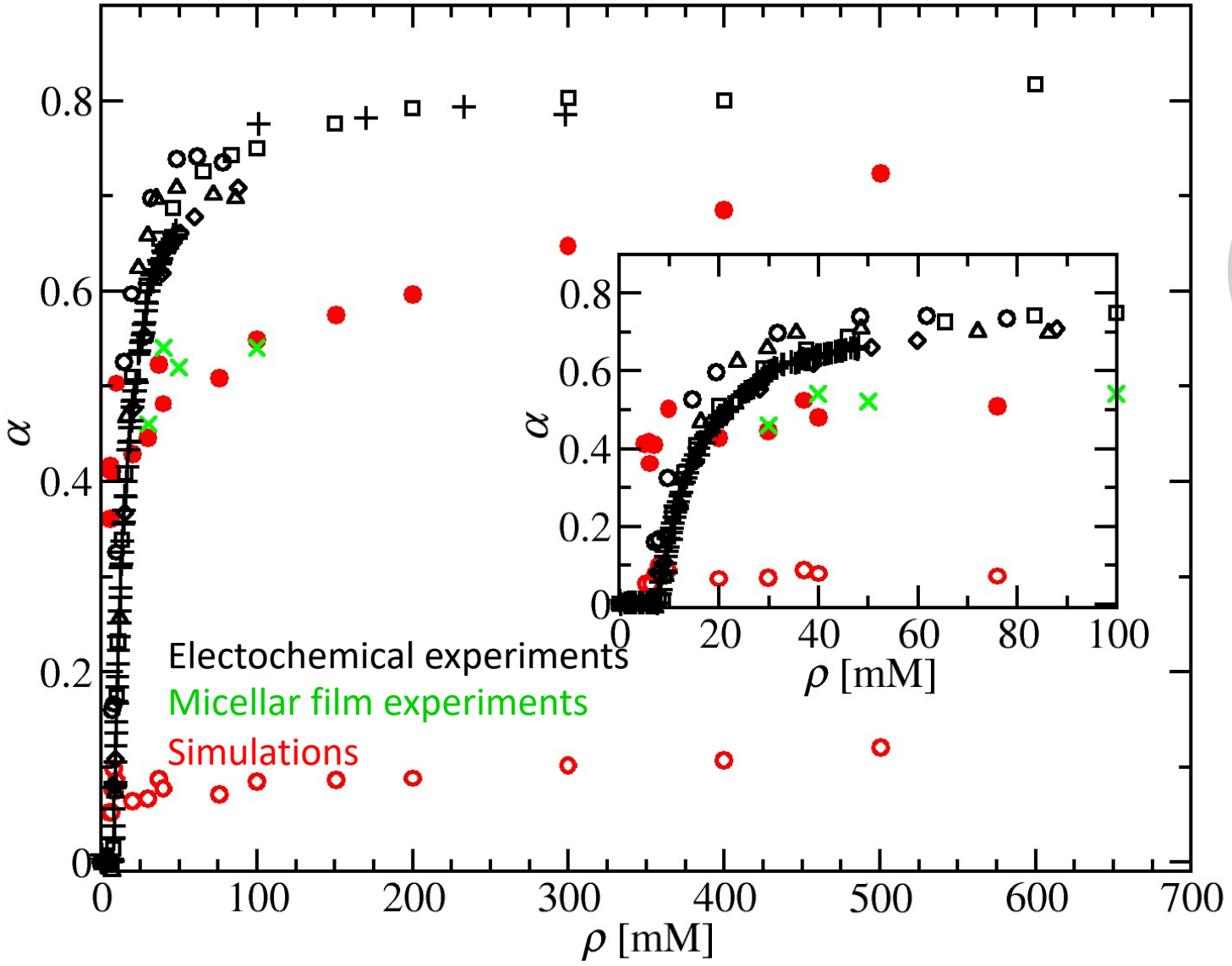

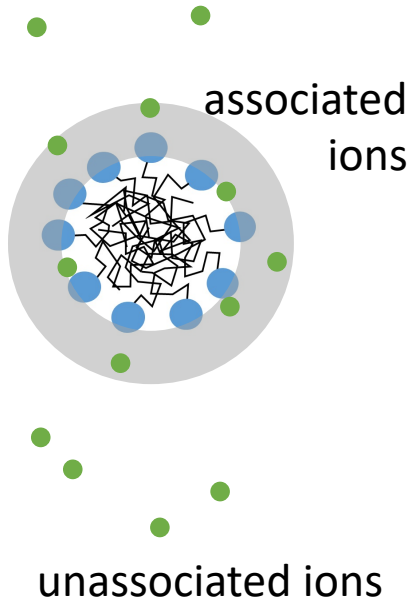

Sasaki, T., Hattori, M., Sasaki, J., & Nukina, K. (1975). *Bull. Chem. Soc. Japan*, *48*(5), 1397–1403.

Cutler, S. G., Meares, P., & Hall, D. G. (1978). *J. Chem. Soc., Faraday Trans. 1*, *74*, 1758–1767.

Kale, K. M., Cussler, E. L., & Evans, D. F. (1980). *J. Phys. Chem.*, *84*(6), 593–598.

Hsiao, C. C., Wang, T.-Y. Y., & Tsao, H.-K. K. (2005). *J. Chem. Phys.*, *122*(14).

Anachkov, S. E., … Ananthapadmanabhan, K. P. (2012). *Adv. Colloid Interface Sci.*, *183–184*, 55–67.

Degree of counterion association

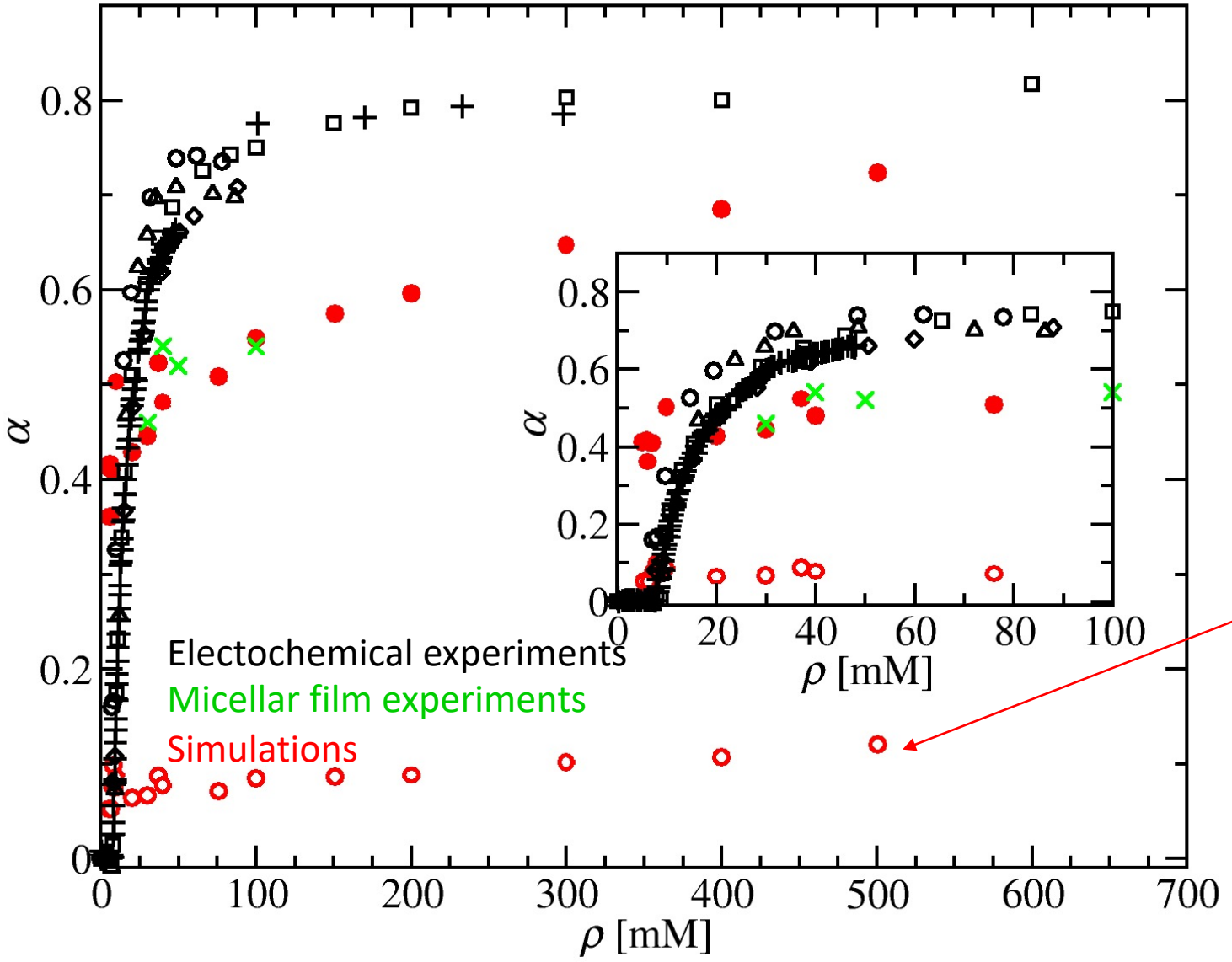

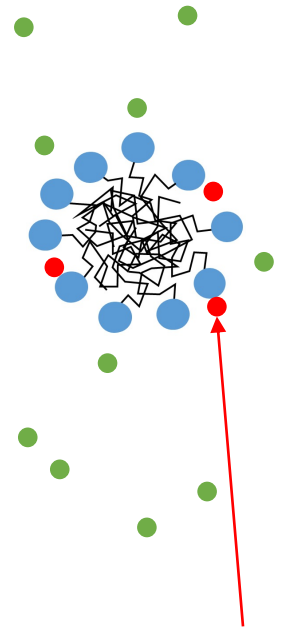

Sasaki, T., Hattori, M., Sasaki, J., & Nukina, K. (1975). *Bull. Chem. Soc. Japan*, *48*(5), 1397–1403.

Cutler, S. G., Meares, P., & Hall, D. G. (1978). *J. Chem. Soc., Faraday Trans. 1*, *74*, 1758–1767.

Kale, K. M., Cussler, E. L., & Evans, D. F. (1980). *J. Phys. Chem.*, *84*(6), 593–598.

Hsiao, C. C., Wang, T.-Y. Y., & Tsao, H.-K. K. (2005). *J. Chem. Phys.*, *122*(14).

Anachkov, S. E., … Ananthapadmanabhan, K. P. (2012). *Adv. Colloid Interface Sci.*, *183–184*, 55–67.

Degree of counterion association

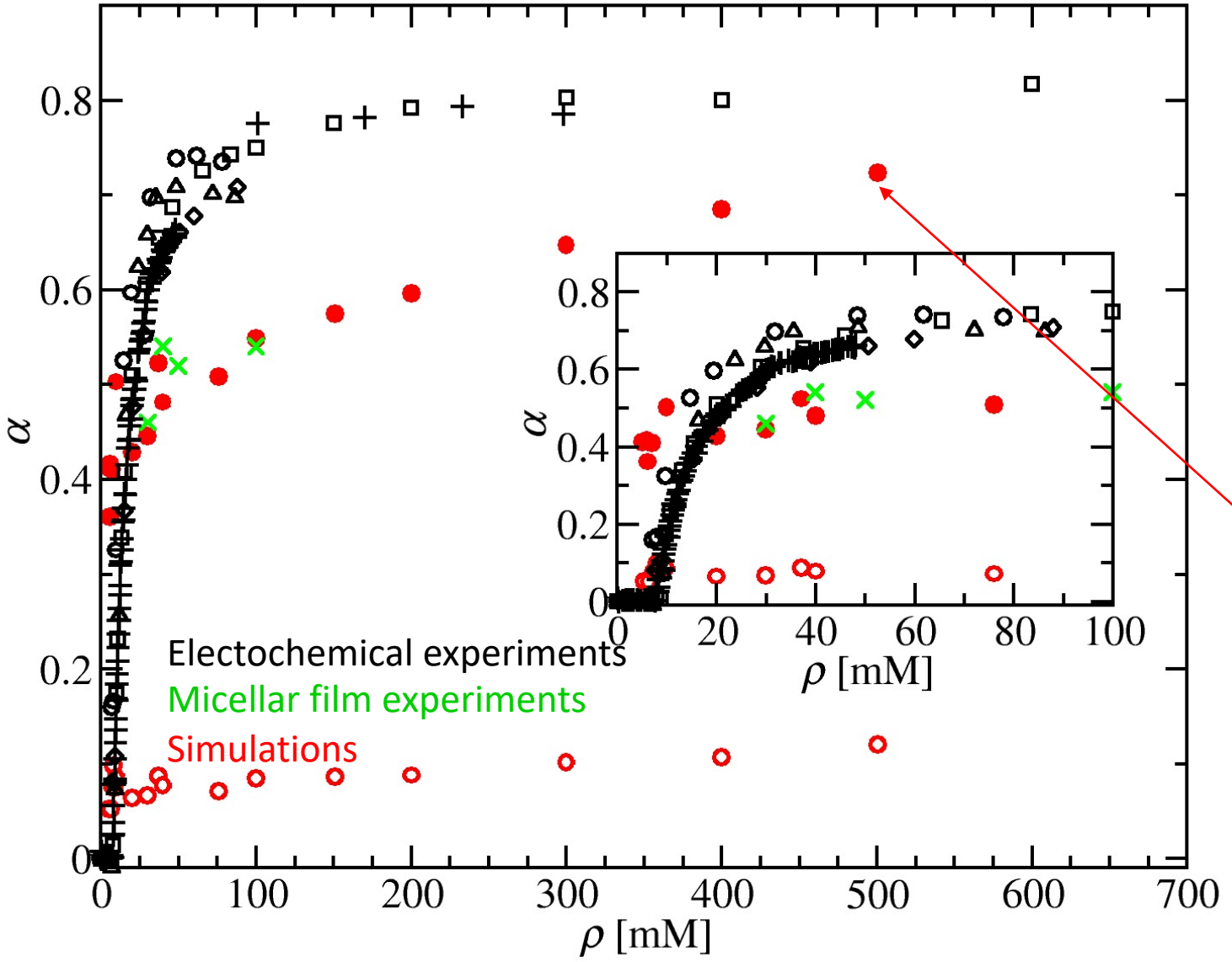

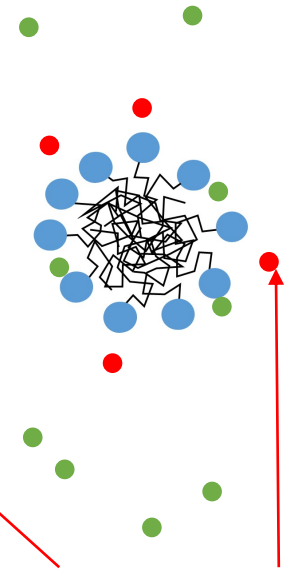

1st hydration shell ions

Sasaki, T., Hattori, M., Sasaki, J., & Nukina, K. (1975). *Bull. Chem. Soc. Japan*, *48*(5), 1397–1403.

Cutler, S. G., Meares, P., & Hall, D. G. (1978). *J. Chem. Soc., Faraday Trans. 1*, *74*, 1758–1767.

Kale, K. M., Cussler, E. L., & Evans, D. F. (1980). *J. Phys. Chem.*, *84*(6), 593–598.

Hsiao, C. C., Wang, T.-Y. Y., & Tsao, H.-K. K. (2005). *J. Chem. Phys.*, *122*(14).

Anachkov, S. E., … Ananthapadmanabhan, K. P. (2012). *Adv. Colloid Interface Sci.*, *183–184*, 55–67.

Full correction

$$\rho_{\text{Bales}} = \exp\left[\frac{1}{(1+\alpha)}\left(\ln \rho_{\text{free}} + \alpha \ln\left(\frac{(1-\alpha)(\rho-\rho_{\text{free}})+\rho_{\text{free}}}{V_{\text{accessible}}}\right)\right)\right]$$

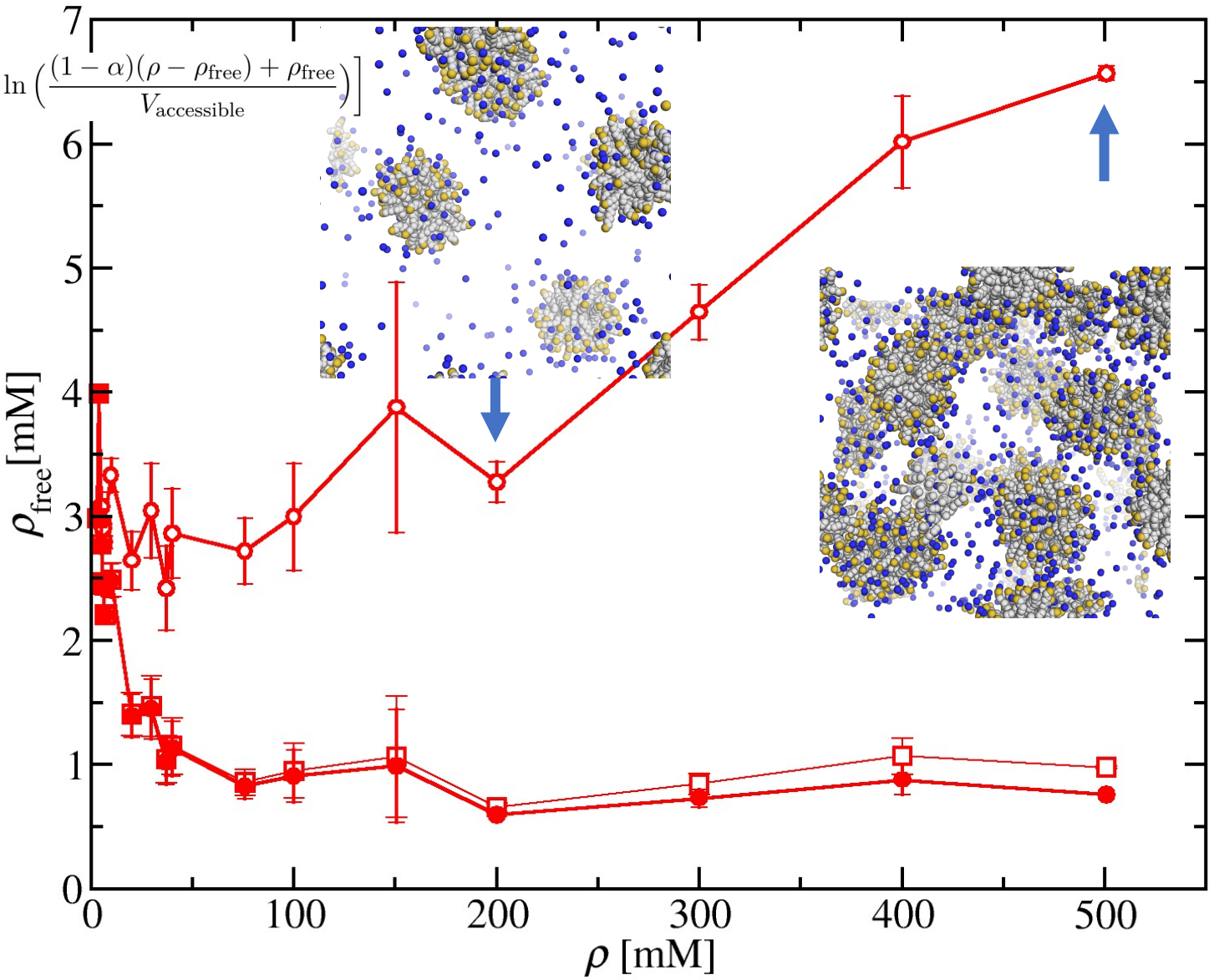

Second critical micelle concentration

Surfactant activity

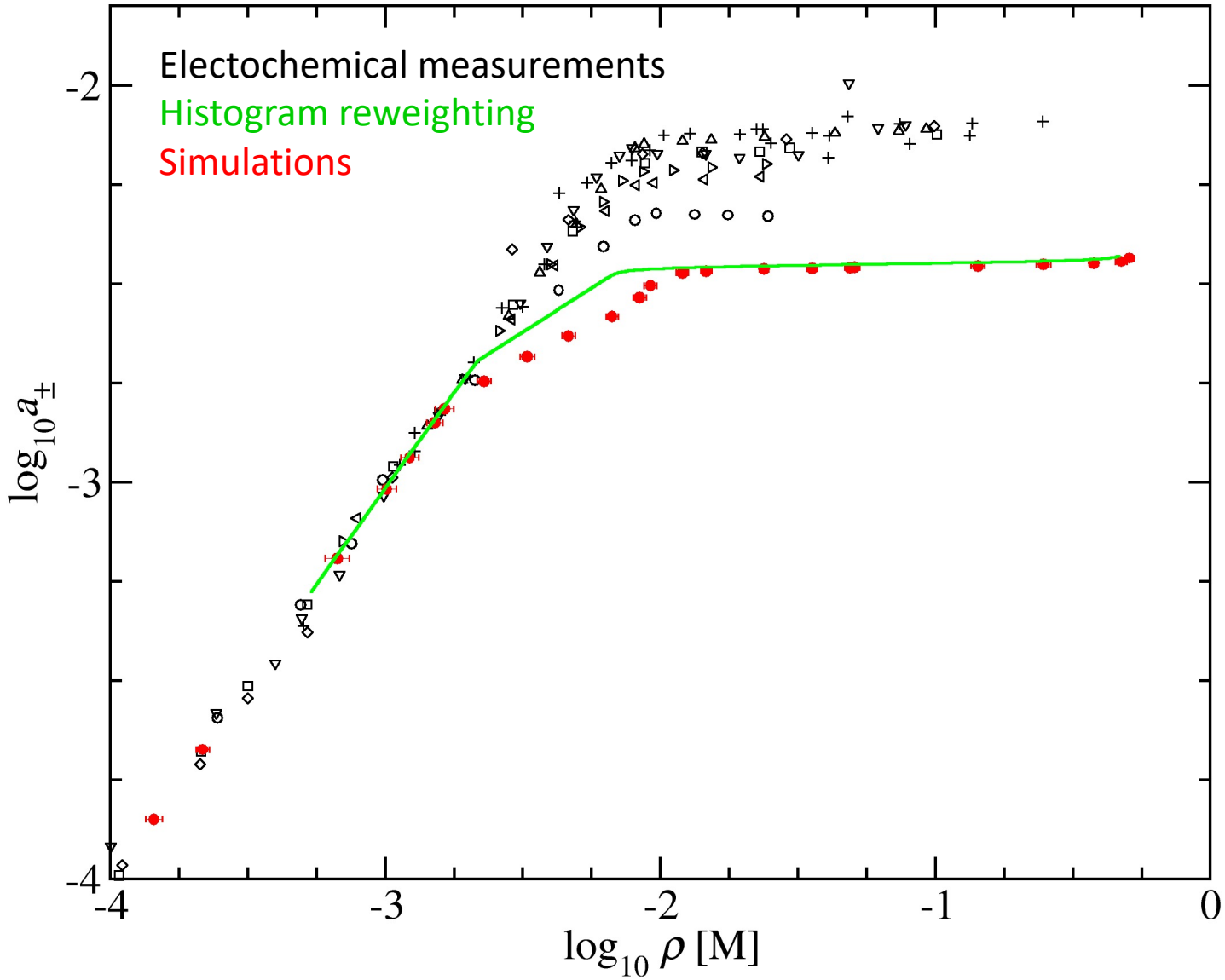

CMC measured by activity

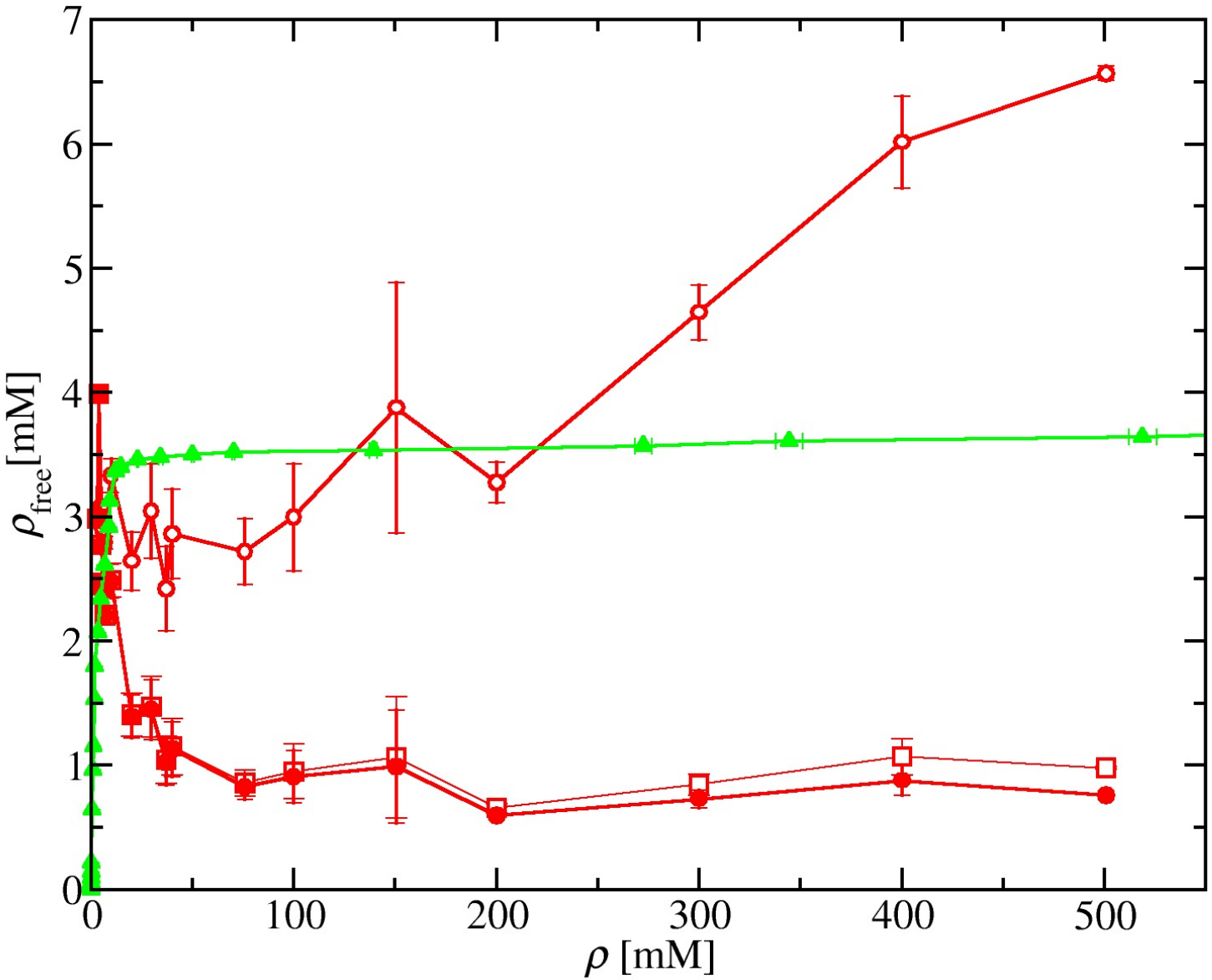

Summary – Ionic Surfactants

- The **inaccessible volume** and **counter-ion condensation** leads to the decrease of the free surfactant concentration for **ionic surfactants**
- The **mean ionic activity** predicts the cmc and the behavior is captured by the model
- The CMC extrapolation is effective at concentrations below higher-order micellar effects

Materials

Surfactants

nonionic

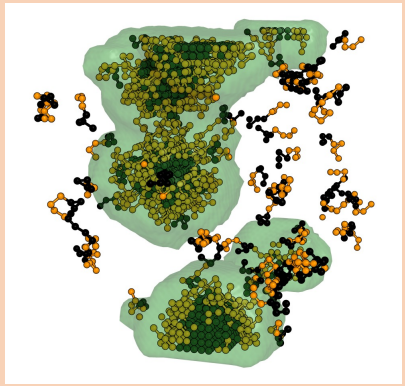

ionic

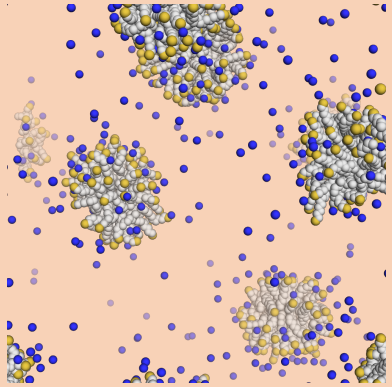

Colloids

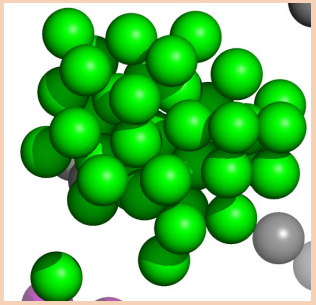

Nanocomposites

Grafted-NP

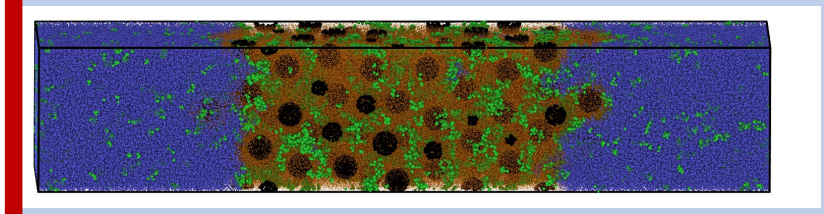

Magnetic

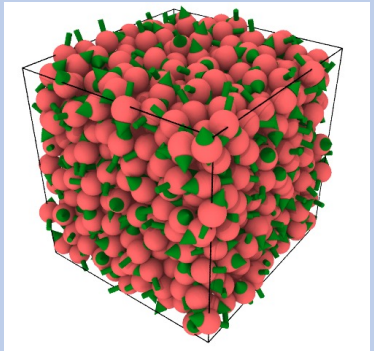

Bare NPs

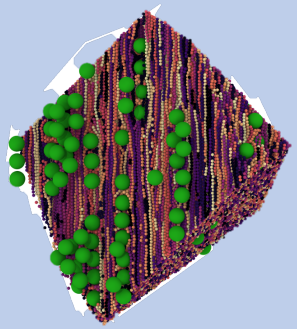

Granular

Packings

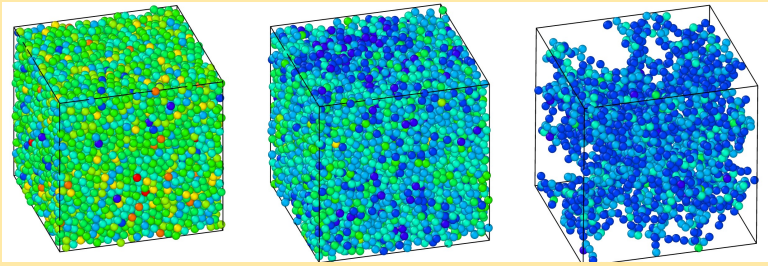

Flow

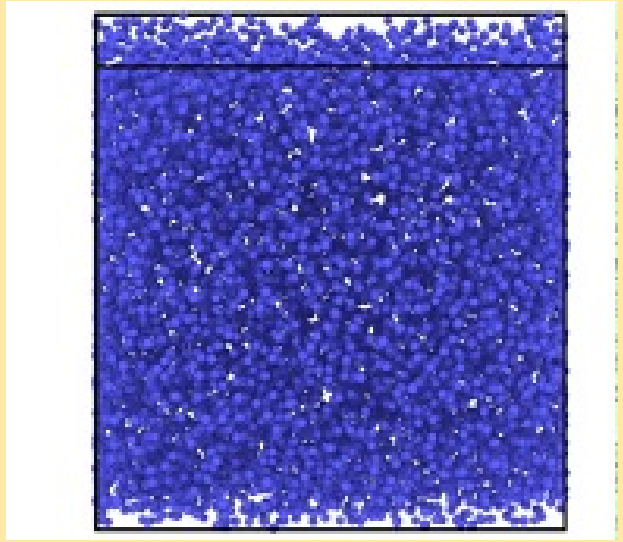

Actualizing Nanocomposites

Application

- Sensors (nanoantennae)
- Stronger materials (filled rubbers)
- Filtration (membranes)

Goal

- Combine the properties from each component (nanoparticles NPs and polymer):
  - Photonic
  - Mechanical
  - Electrical
  - Magnetic

Challenges

- Design can control final nanoparticle morphology.
- Morphology dominates properties and applicability.
- Limited molecular solvent-polymer-grafted nanoparticle phase coexistence data

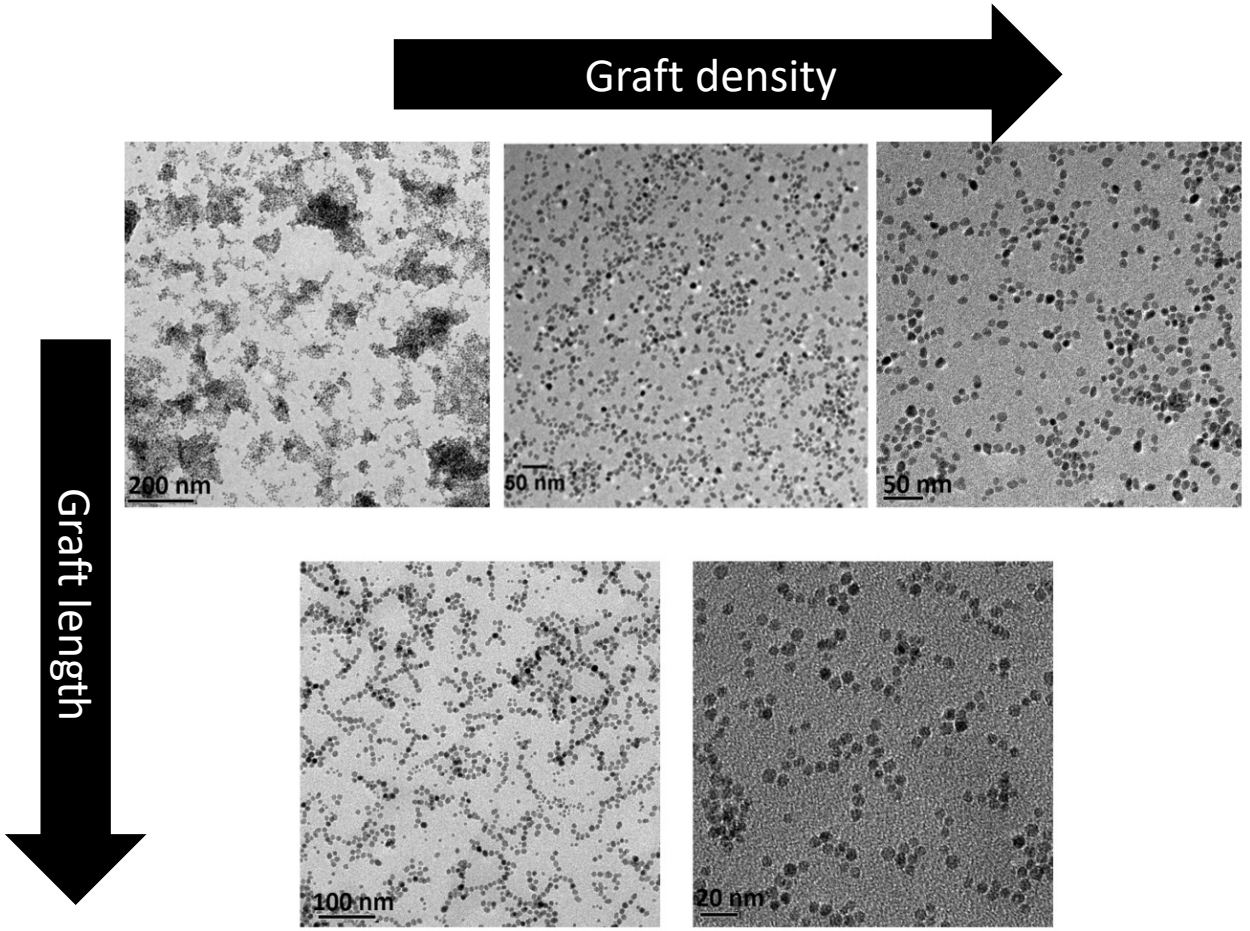

Mongcopa, K. I. S., *et al*. (2018). *Soft Matter*, *14*(29), 6102–6108.
Bachhar, N., *et al*. (2017). *Macromol.*, *50*, 7730–7738.

Nanocomposite systems overview

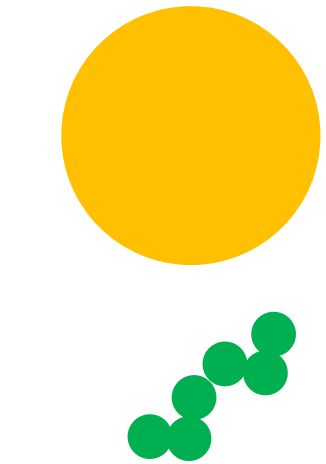

grafted NPs in polymer

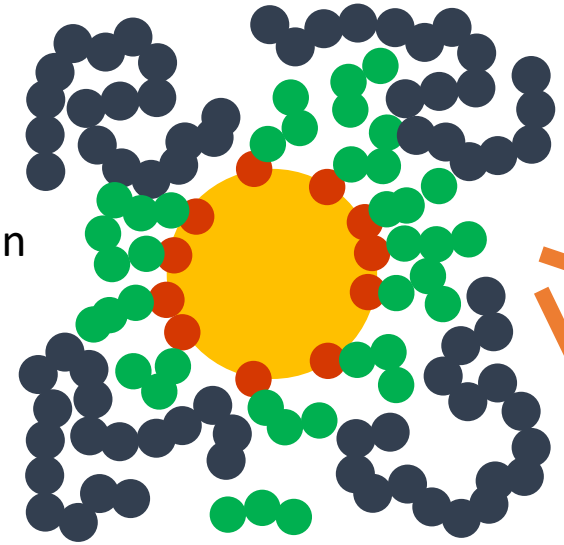

Control nancomposite properties

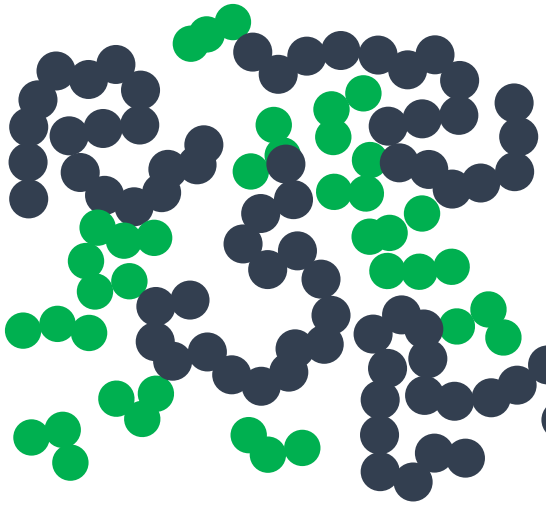

number of component

graft density

Bare NPs & polymer

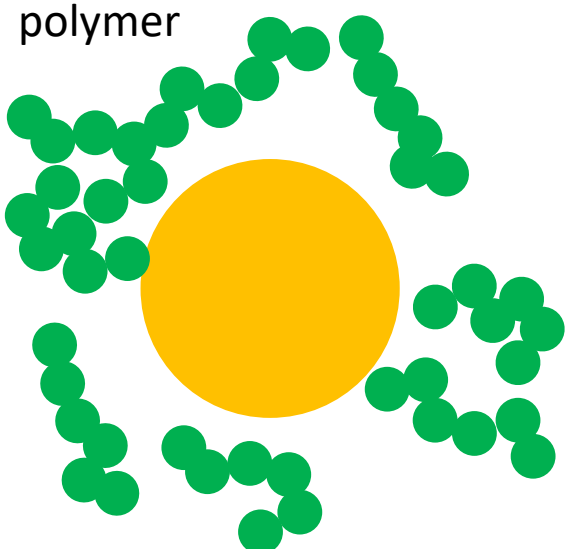

grafted NPs in solvent

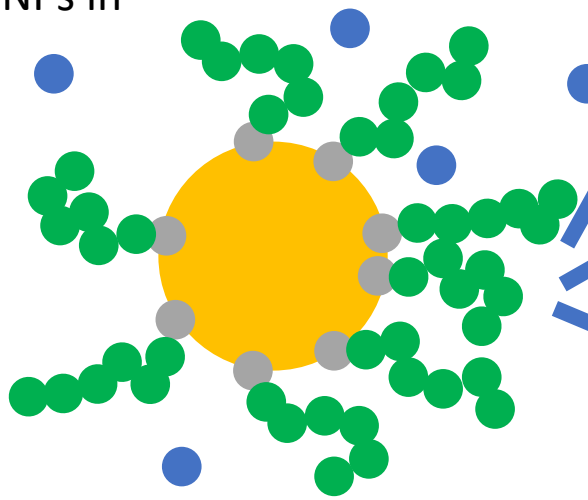

interaction strength (or temperature)

graft length

NP size

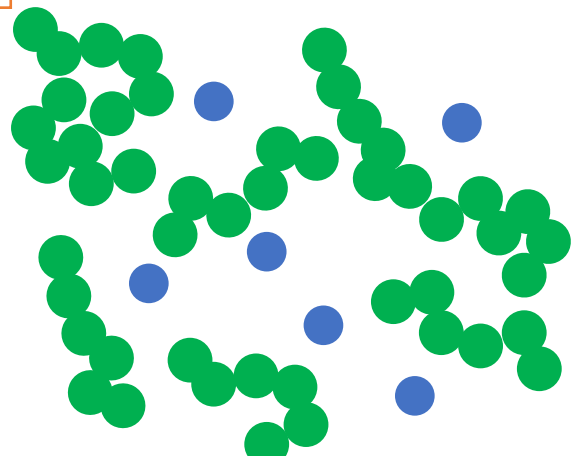

Experimental solvent system (PS-g-Au in cyclohexane)

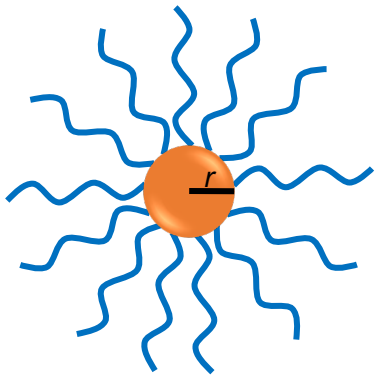

Filled Symbols:
r = 10nm
N = 215, 268, 314, and 530

Open Symbols:
r = 6nm
N = 268, 314, and 530

- UV-vis spectroscopy
- SAXS

- Polymer grafted-NPs (PGNs) differ from stars

- Higher PGN miscibility is observed for lower N
- Similar miscibility at different core sizes

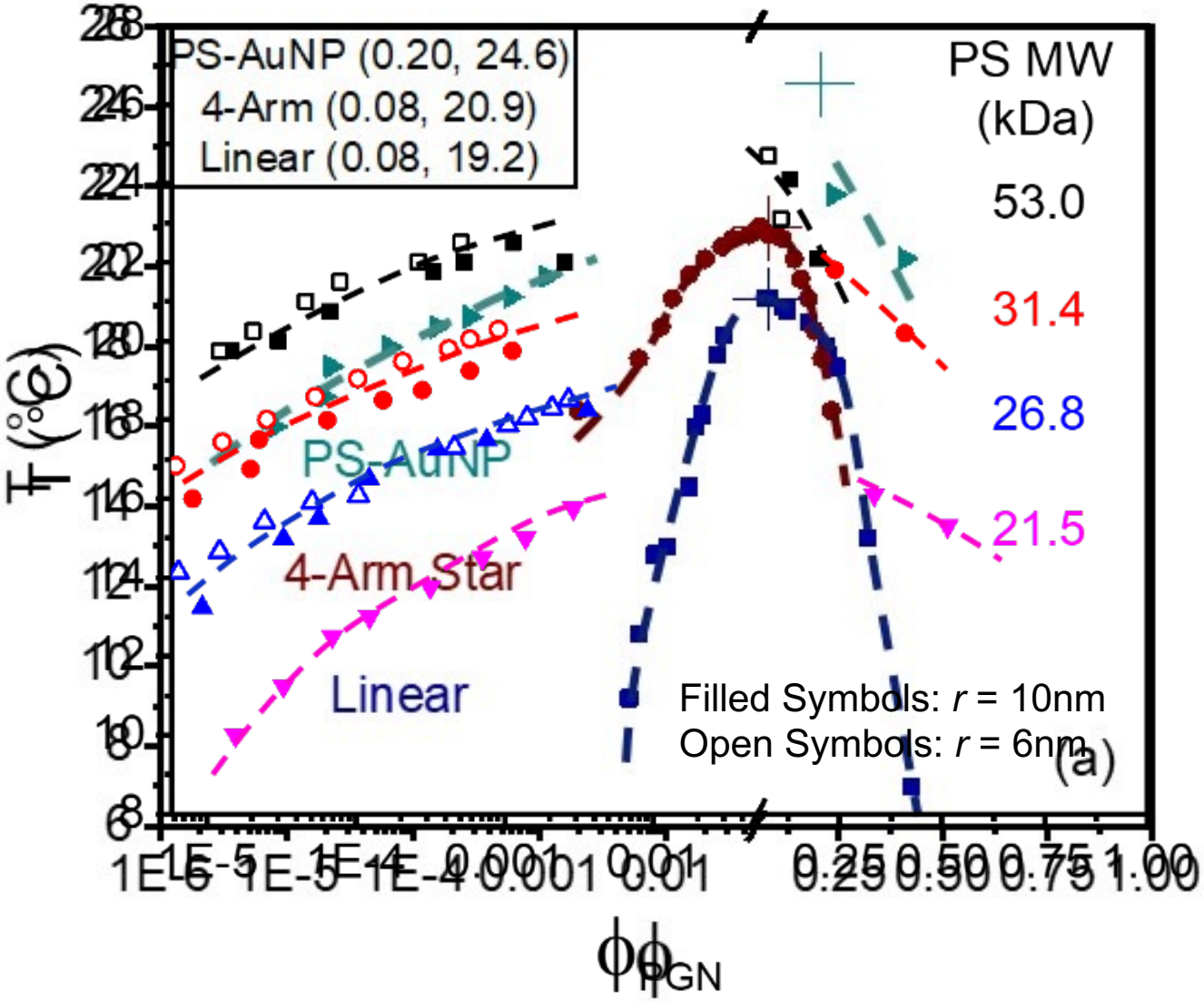

Sarah N. Izor, Allen B. Schantz and Richard A. Vaia at Air Force Research Laboratory

Coarse-graining solvent system

Experimental to Simulation system

1. Pick graft length (N_G) for convenience
2. By matching reduced grafting density (σ*) get density (ρ_0), length (b) and nanoparticle radius (R_{NP})

System property	Experimental	TILD simulations
NP radius	10, 6 nm	7.47, 4.48 b
Graft mol. weight	21.5 kDa	51 beads
	26.8 kDa	63 beads
	31.4 kDa	74 beads
	53 kDa	126 beads
Grafting density	1.01-0.59 chains/nm^2	0.18 chains/b^2 (266-2462 chains/NP)

match grafting density

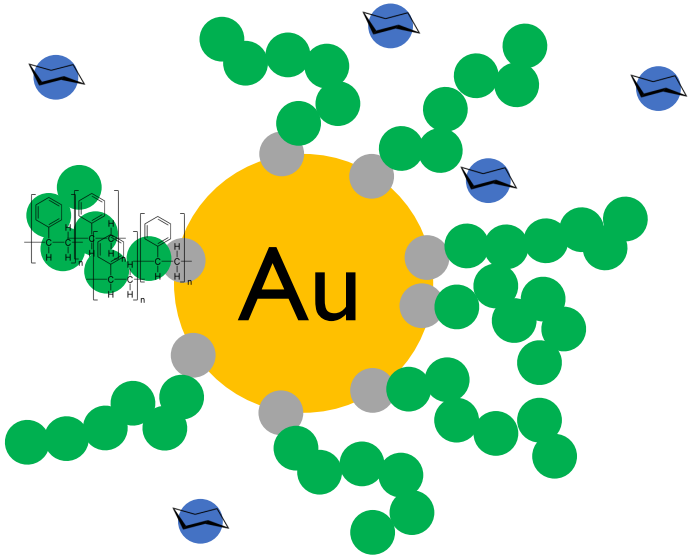

Polystyrene-grafted gold nanoparticles in cyclohexane

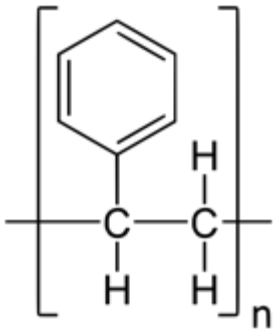

Au

Chao, H., Koski, J., & Riggleman, R. A. (2017). *Soft Matter*, *13*(1), 239–249.

Theoretically-informed Langevin Dynamics (TILD)

Method	TILD	Self-consistent mean field (SCMF)	Coarse-grained MD
Easy access to free energy			
Accurate dynamics			
Thermal fluctuations			
Accurate solvent modeling			
Field theory comparison			
Long polymers and multiple NPs			

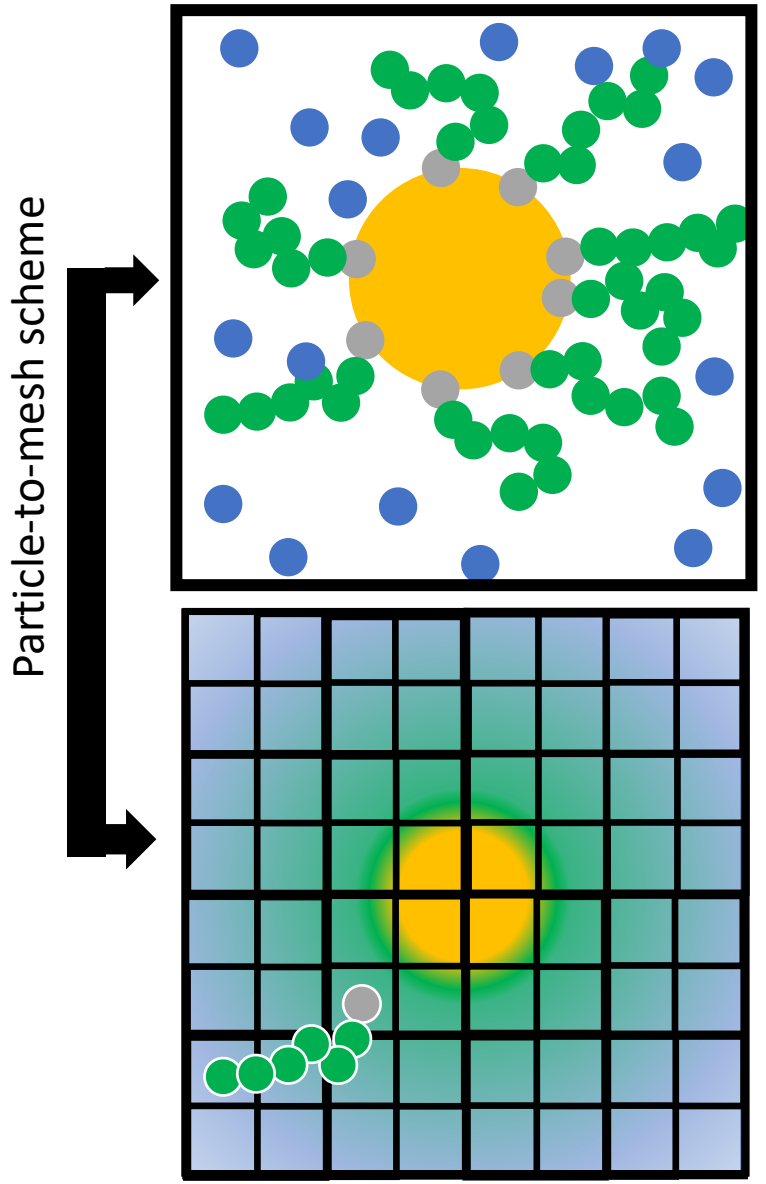

Procedure

- Molecular Dynamics evolves simulation of soft, point-based particles using 2nd Law, in the *NVT* ensemble
- *T* is controlled with Langevin thermostat
- Force on each particle is calculated by field-based interaction

Chao, H., Koski, J., & Riggleman, R. A. (2017). *Soft Matter*, *13*(1), 239–249.
Martin, T. B., & Jayaraman, A. (2016). *Macromolecules*, *49*(24), 9684–9692.
Koh, C., Grest, G. S., & Kumar, S. K. (2020). *ACS Nano*, *14*(10), 13491–13499.

Theoretically-informed Langevin Dynamics (TILD)

Parameters

- Nonbonded interaction parameters
  - Inteaction parameter: $\chi_{sol\text{-}mono} = \chi$
  - Compressibility: κ=25
  - Otherwise nanoparticles are non-interacting
- Harmonic bonds
  - k_{bond} = 1.5

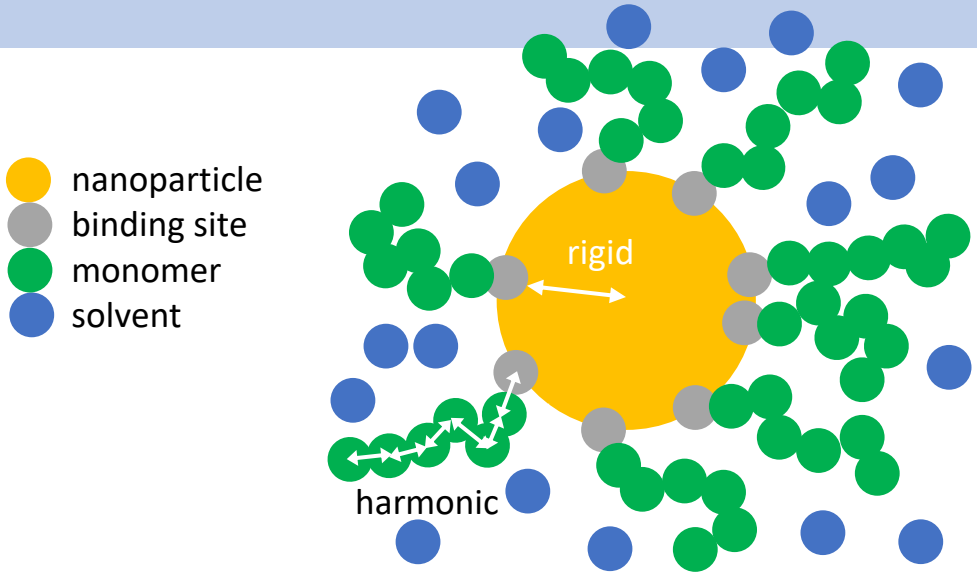

- Langevin Gronbech-Jensen/Farago formulation thermostat applied to polymer and solvent
  - T = 1, $T_{damp}^{trans} = T_{damp}^{rot} = 1$
  - $m_{solvent}=m_{monomer}=1$, $m_{NP}=\rho_0/V_{np}$
- PPPM
  - mesh density = $1b^3$
  - grid order = 2

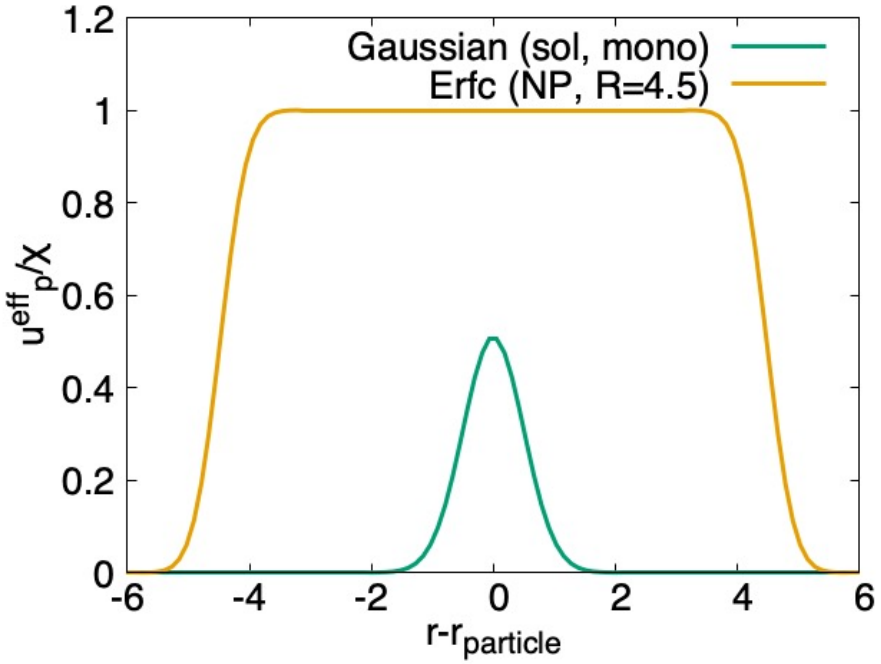

Chao, H., Koski, J., & Riggleman, R. A. (2017). *Soft Matter*, *13*(1), 239–249.
Grønbech-Jensen, N., & Farago, O. (2013). *Mol. Phys.*, *111*(8), 983–991.

Brush profile

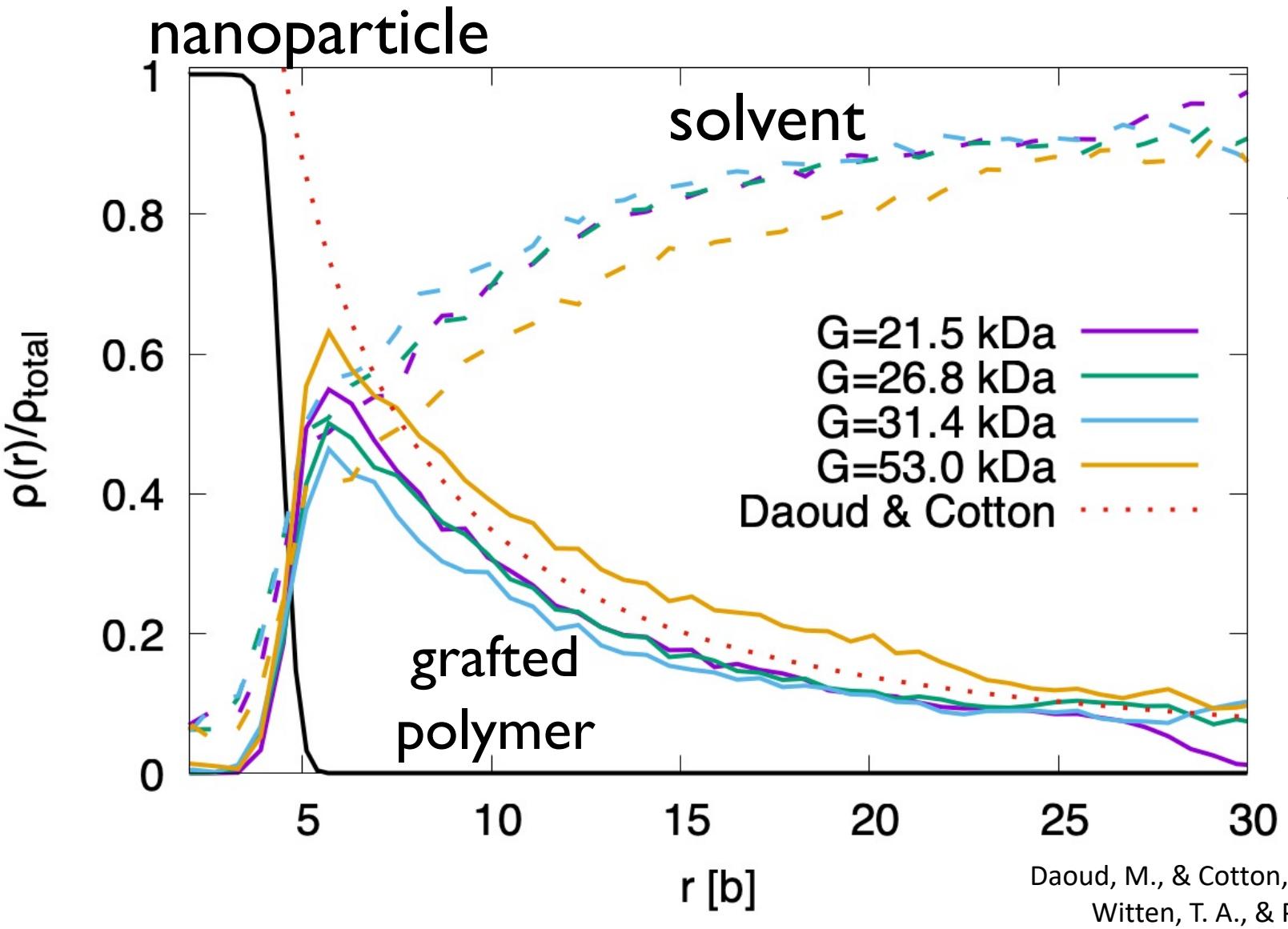

R_{NP}=4.48b (6nm)

χ=0.25

σ = 0.18 chains/b^2

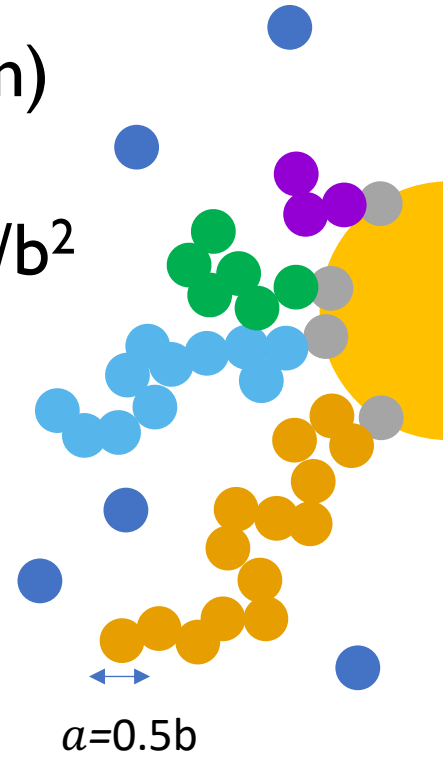

$$\rho_{\text{Daoud-Cotton}}(r) = \left(\frac{aR_{\text{NP}}\sqrt{\sigma}}{r}\right)^{4/3} a^{-3}$$

Daoud, M., & Cotton, J. P. (1982). *J. Phys. France*, *43*(3), 531–538.
Witten, T. A., & Pincus, P. A. (1986). *Macromolecules*, *19*(10)

Direct phase coexistence

Direct coexistence
simulation configuration

Density profile
of each state point, fit gives phase-coexistence

$$\phi_{\mathrm{sol}}(z) = \phi_{\mathrm{sol}} + \frac{\phi_{\mathrm{gNP}} - \phi_{\mathrm{sol}}}{2}\left(\mathrm{erf}\left[\frac{z - L_z/2 + z_0}{\Delta\sqrt{2}}\right] - \mathrm{erf}\left[\frac{z - L_z/2 - z_0}{\Delta\sqrt{2}}\right]\right)$$

fits

Δ Interface width

Phase diagrams
from ϕ_{gNP} and ϕ_{sol} to density profile

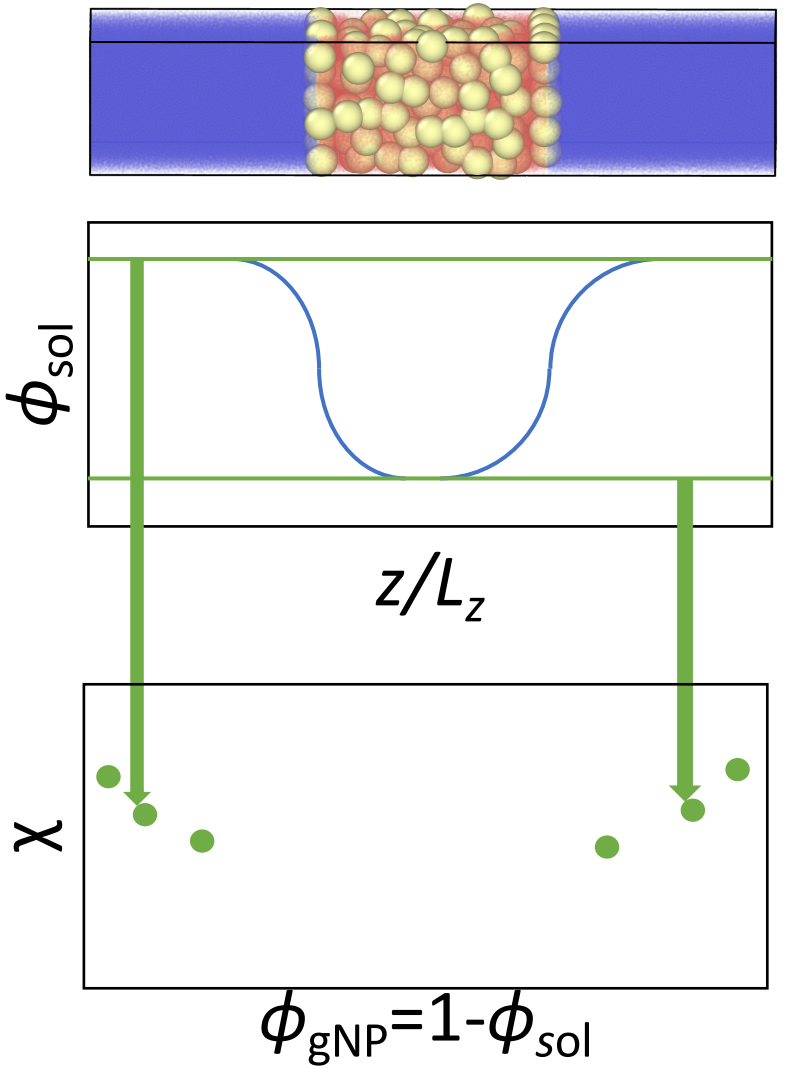

Koski, J. P., et al. (2019). *Macromolecules*, *52*(14), 5110–5121.

Phase behavior

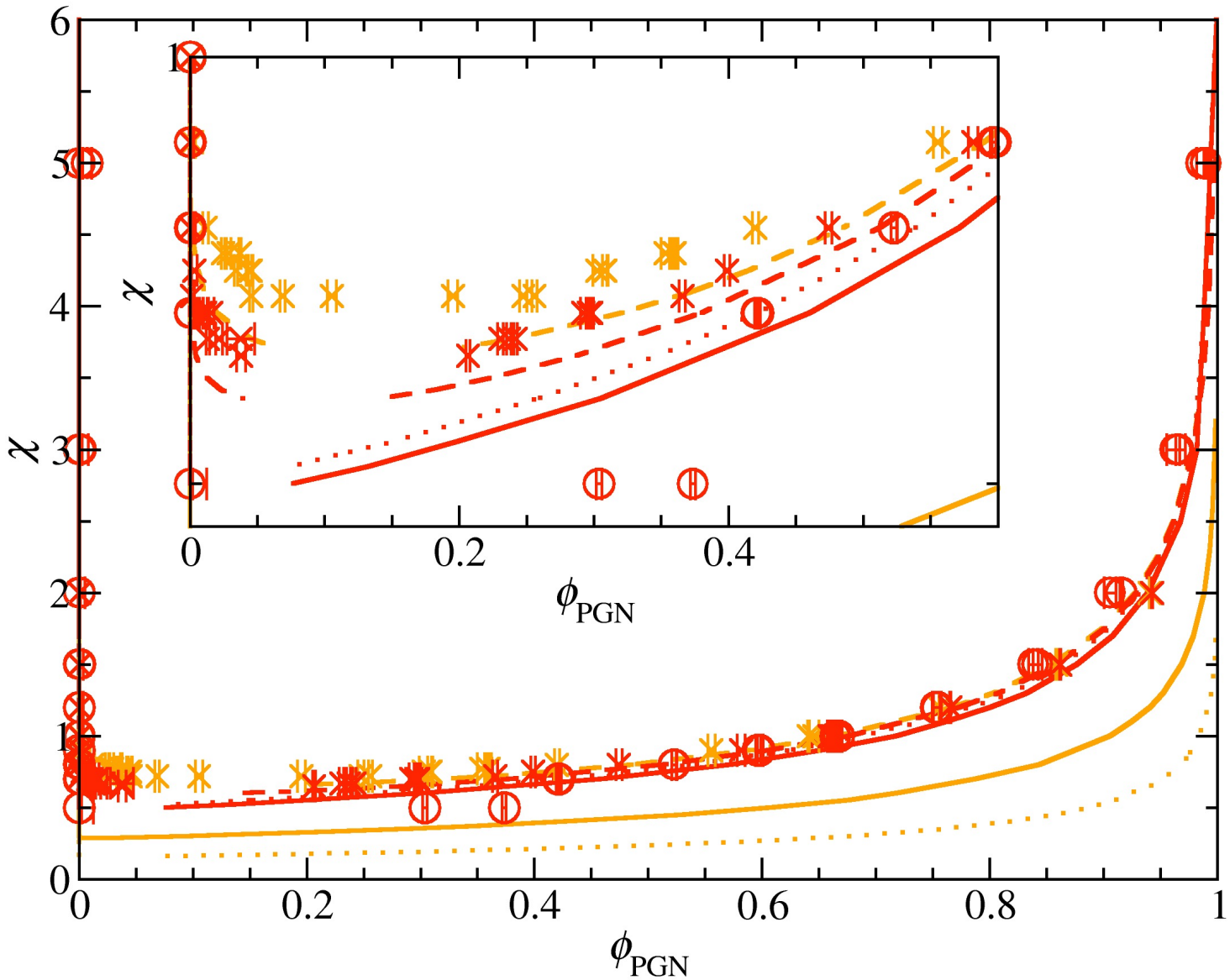

symbols: TILD

star: homopolymer

circle: PGN

lines: Flory-Huggins theory

short graft, N_g=21.5 kDa (51 beads)

long graft N_g=53 kDa (126 beads)

Koski, J. P., … Riggleman, R. A. (2019). *Macromolecules*, *52*(14), 5110–5121

Summary – GNPs in solvent

- Graft radial density profile obeys Dauod & Cotton
- Flory-Huggins better predicts homopolymer than PGN phase behavior
- Our method equilibrates long polymers in tractable times
- Nanoparticle size has little effect on phase separation
- Phase separation is induced by:
    1. Increasing polymer-solvent interaction
    2. Increasing grafted polymer length

Experimental homopolymer blend system (PMMA-g-SiO_2 in SAN/PMMA)

PMMA

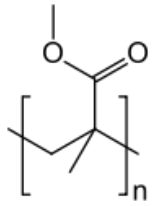

SAN

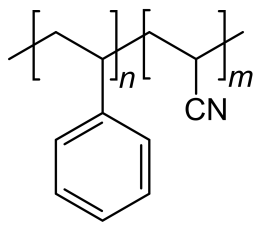

Poly(methyl methacrylate)-grafted Silica Nanoparticles in poly(styrene-co-acrylonitrile) [33% AN]

- Optical turbidity
- TEM
- SAXS

- Phase envelope opens with ternary component
- Interfacial compatibilization

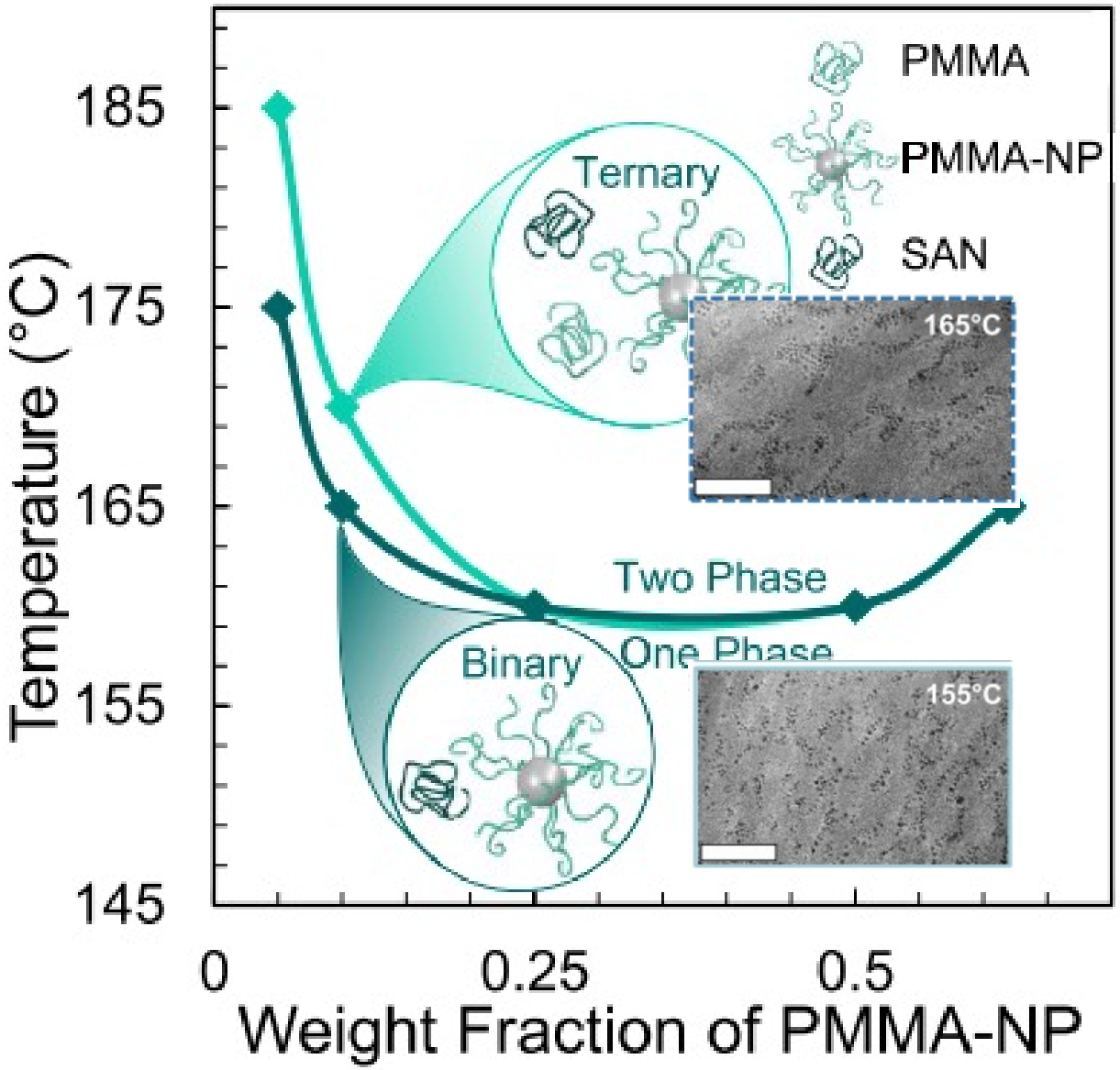

Maguire, S. M., Krook, N. M., …, Jayaraman, A., Composto, R. J. (2021) *Macromolecules*, *54*(2), 797–811.

Coarse-graining homopolymer blend system

Property	Experimental	TILD
N_G	19 kDa	17
N_M	118 kDa	123
ρ_0		3.41
b		2.29 nm
σ	0.7 chains/nm^2	3.69 chains/b^2 (0.27 chains/nm^2)
R_{np}	7.5 nm	3.27 b (7.5 nm)

binary

$\phi_{PMMA\text{-}m}=0$

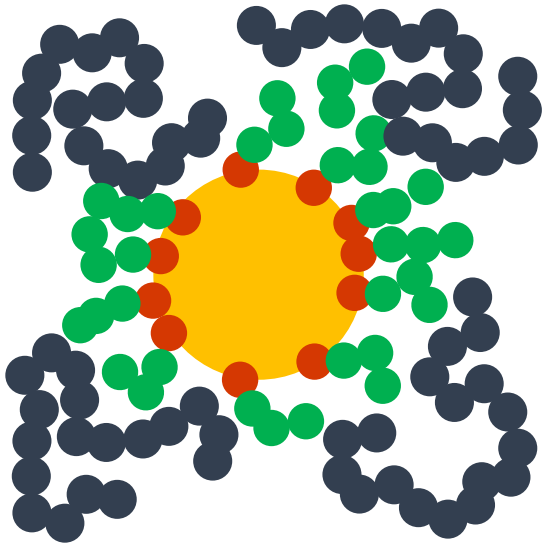

ternary

$\phi_{PMMA\text{-}m}=0.1$

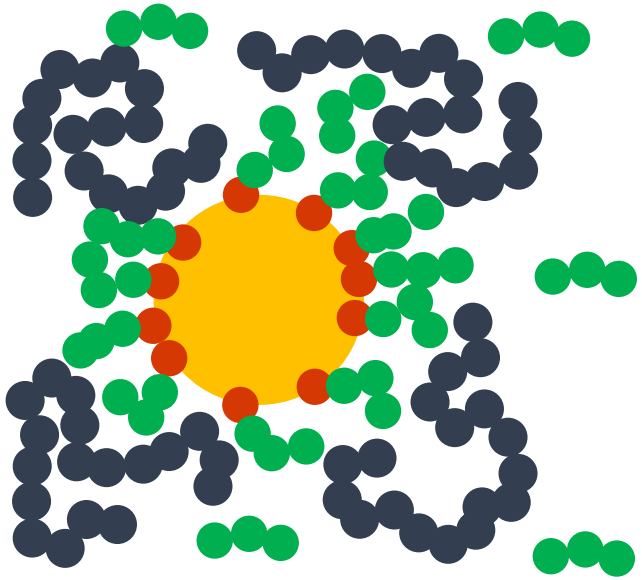

PMMA and SAN (33% Nitrile) ρ, *b* and χ from:

Aoki et al. Macromolecules, 52, 3, 1112-1124 (2019). 10.1021/acs.macromol.8b02431

Phase behavior

Homopolymer blend

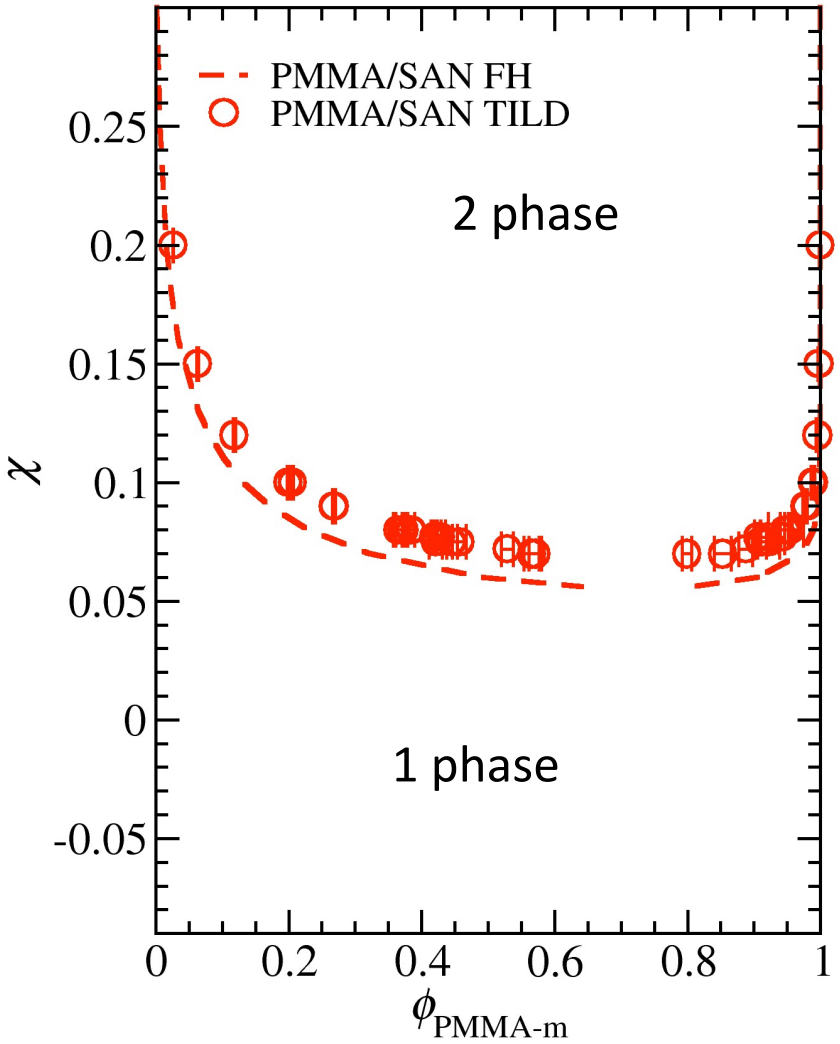

Polymer-grafted nanoparticles

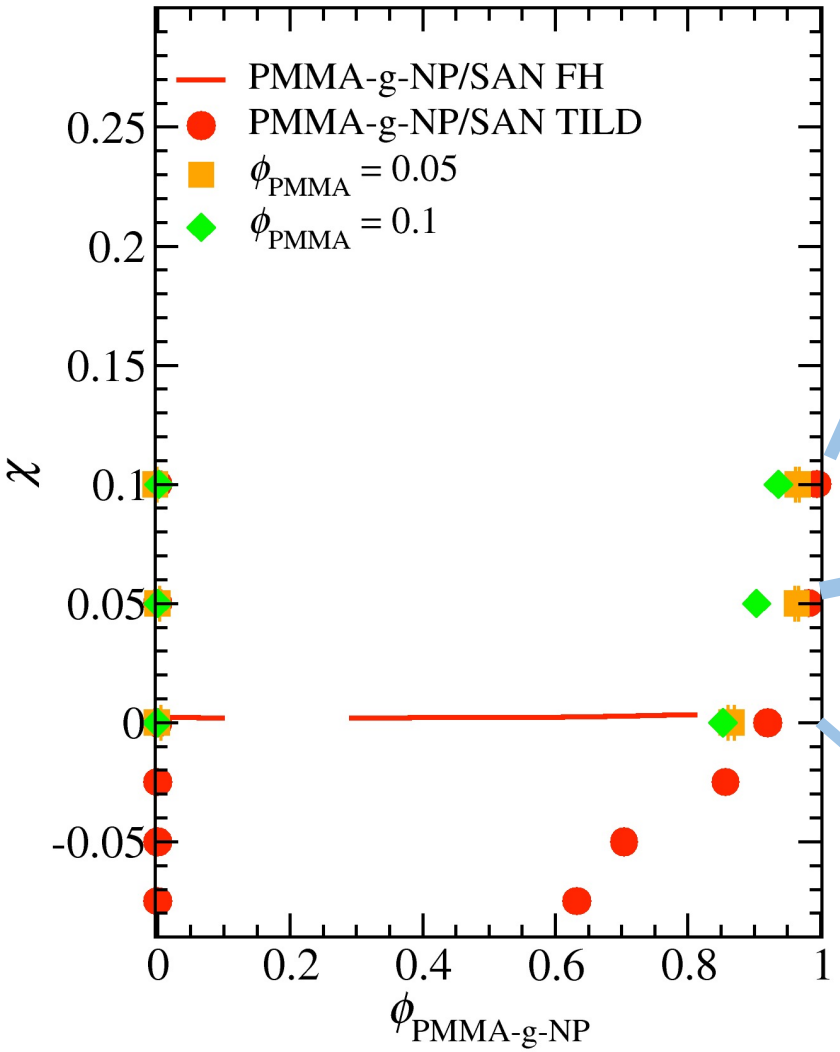

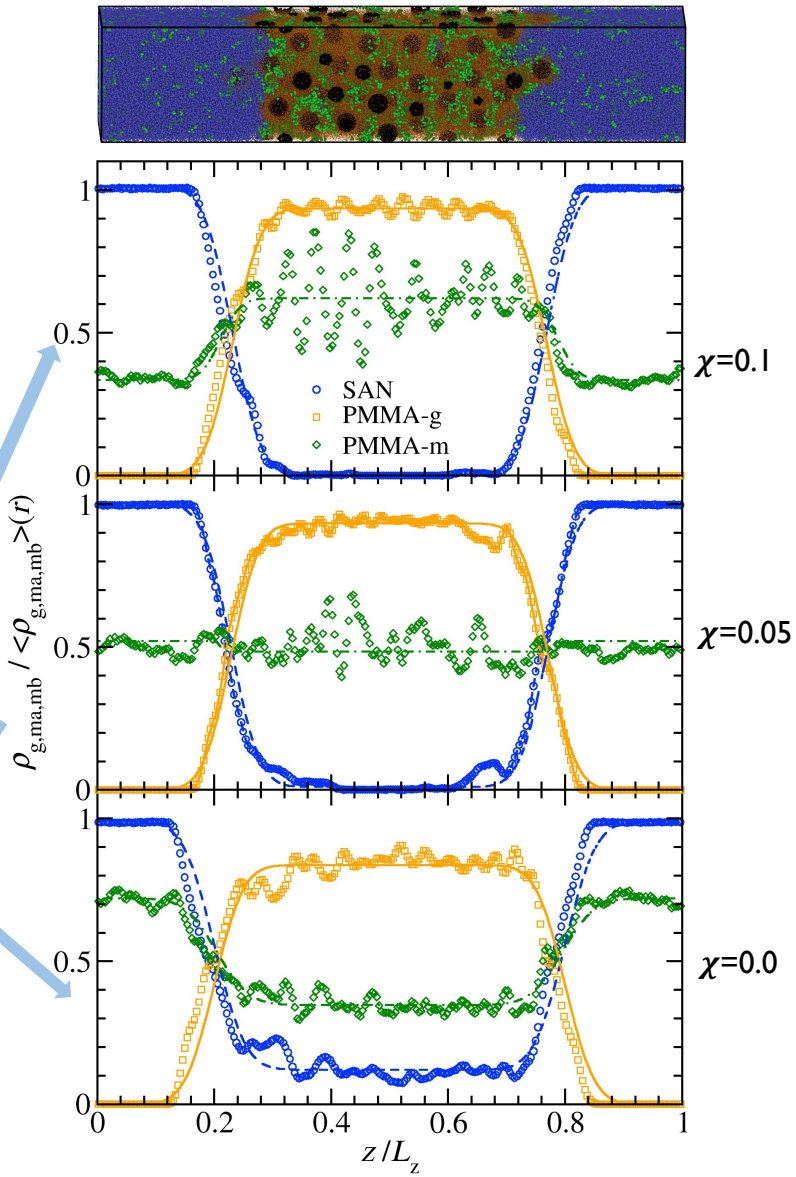

PGN brush profile

Polymer-grafted nanoparticles

$\phi_{\text{PMMA-m}}$

0.05

0.1

0.15

0.2

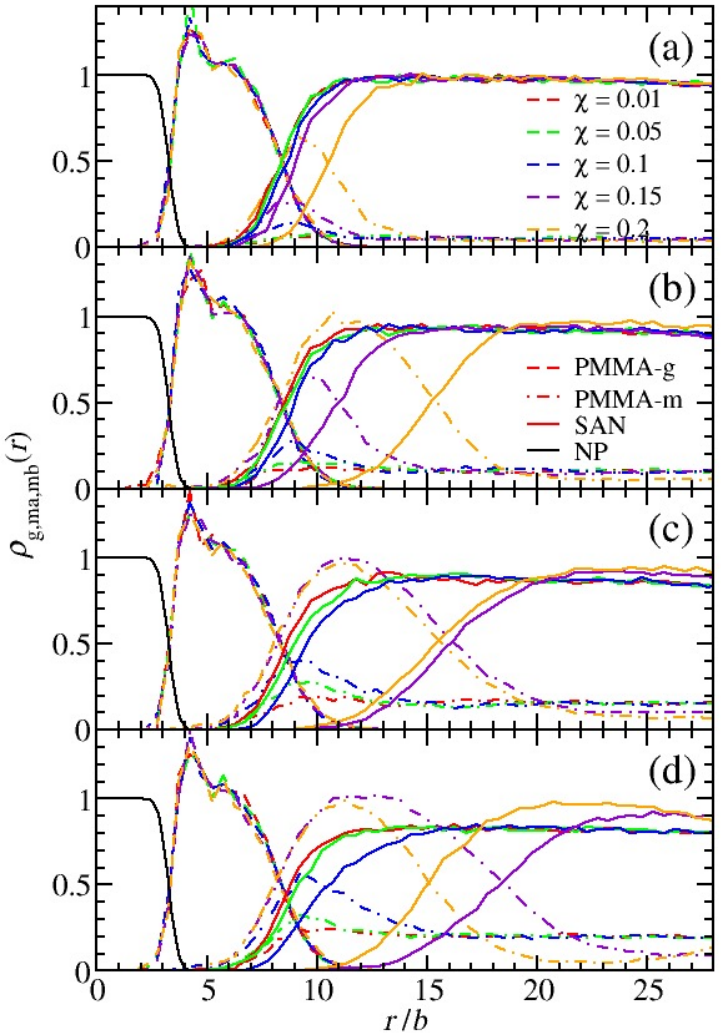

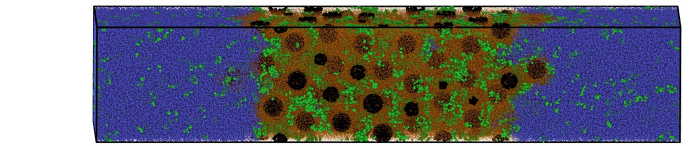

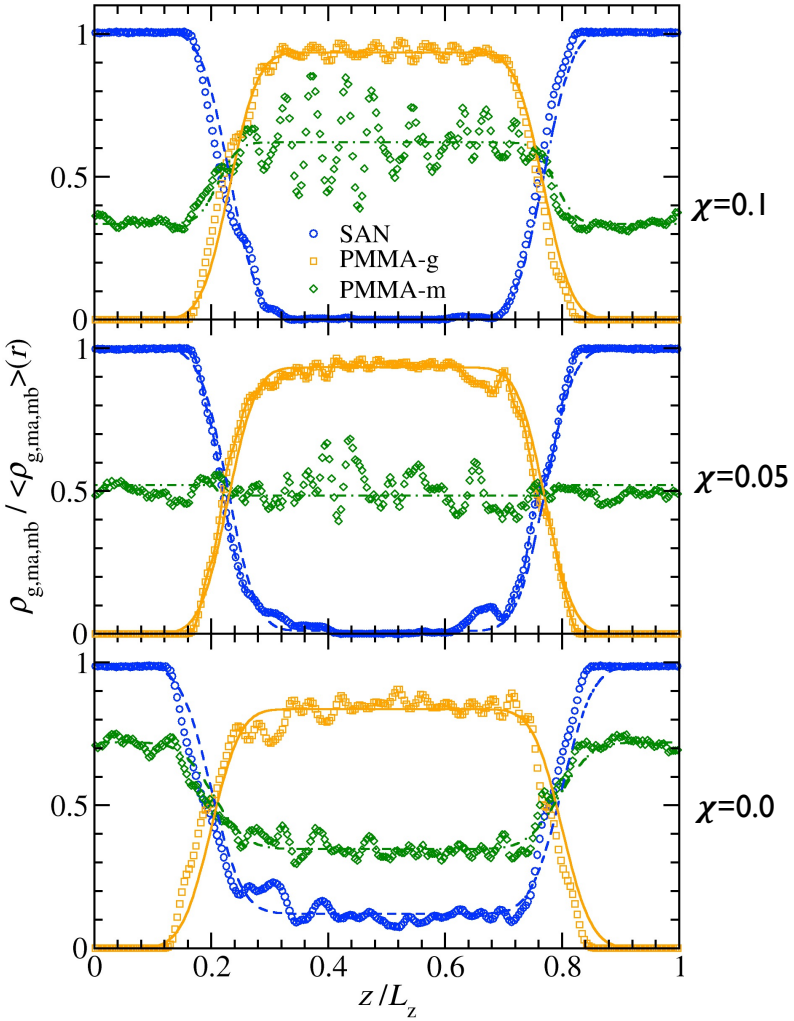

Crystallization

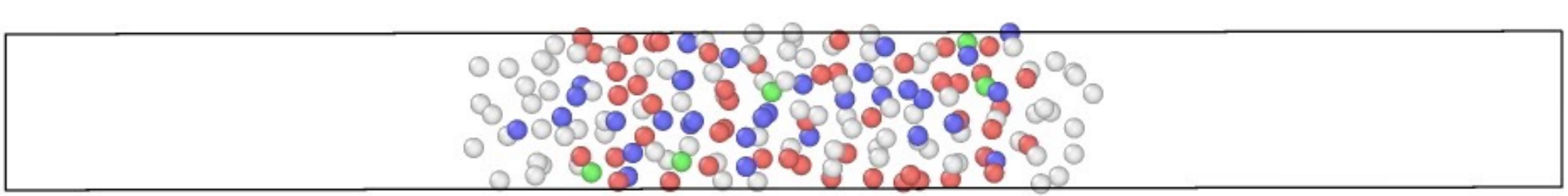

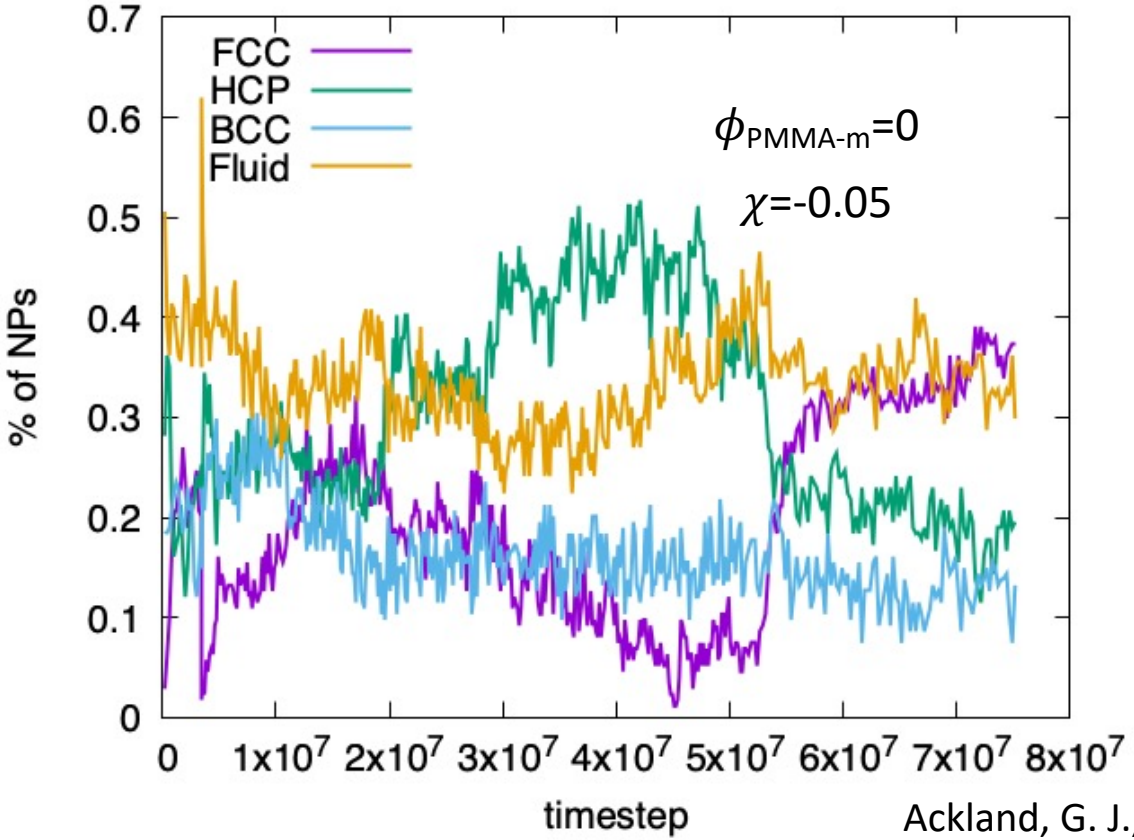

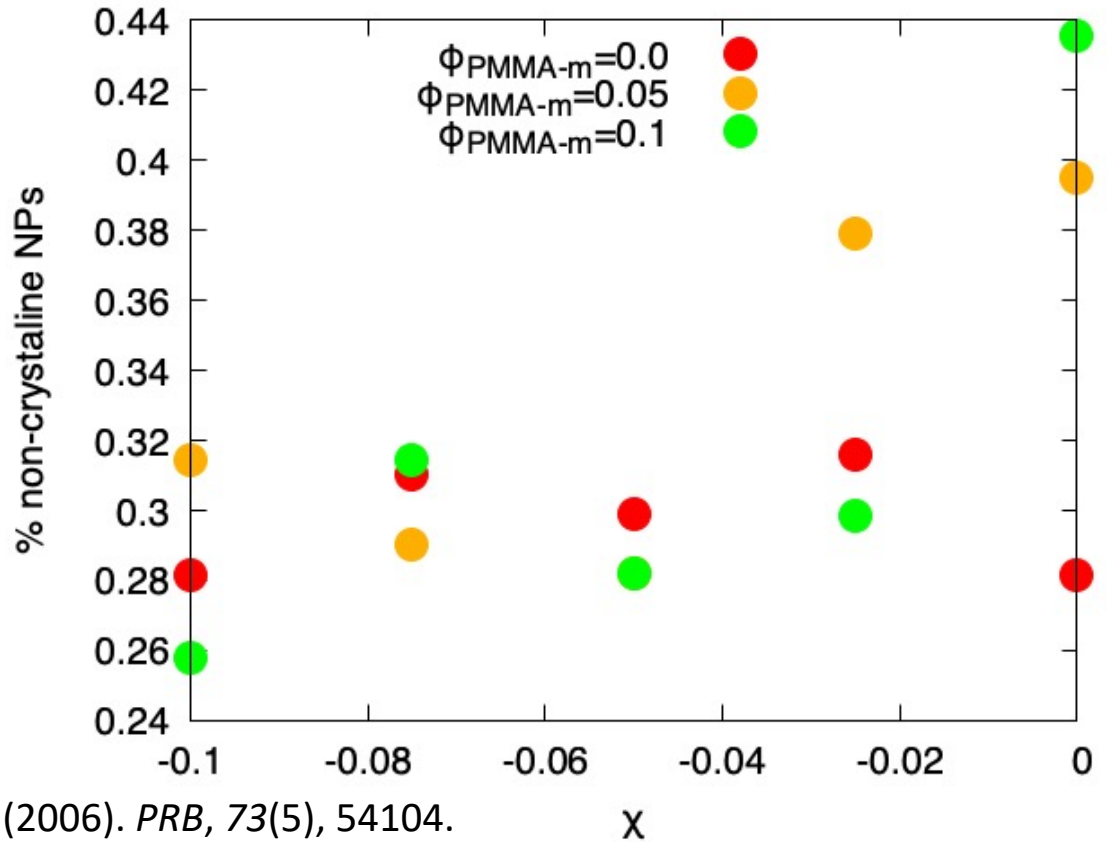

Ackland, G. J., & Jones, A. P. (2006). *PRB*, *73*(5), 54104.

Summary – GNPs in homopolymer

- Nanoparticles order in dense phase
- PMMA/SAN homopolymer phase transition determines:
  - high density of PMMA matrix at graft-melt interface
  - PMMA matrix preference in SAN- or PGN-dense phases
- Flory-Huggins PNC theory does not capture low critical point

Acknowledgments

Amalie L. Frischknecht
Gary Grest
Mark Stevens

Sarah N. Izor
Allen B. Schantz
Richard A. Vaia

Shawn Maguire
Russ Composto

Christian Tabedzki
Rob Riggleman

email: asanto@sandia.gov

Prof. Panagiotopoulos

This work was performed at the Center for Integrated Nanotechnologies, a U.S. Department of Energy and Office of Basic Energy Sciences user facility. Sandia National Laboratories is a multimission laboratory managed and operated by National Technology and Engineering Solutions of Sandia, LLC, a wholly owned subsidiary of Honeywell International, Inc., for the U.S. Department of Energy's National Nuclear Security Administration under Contract No. DE-NA-0003525.

NSF GRFP DGE-1656466
DOE Basic Energy Sciences DE-SC0002128

Radius of gyration (PMMA/SAN)

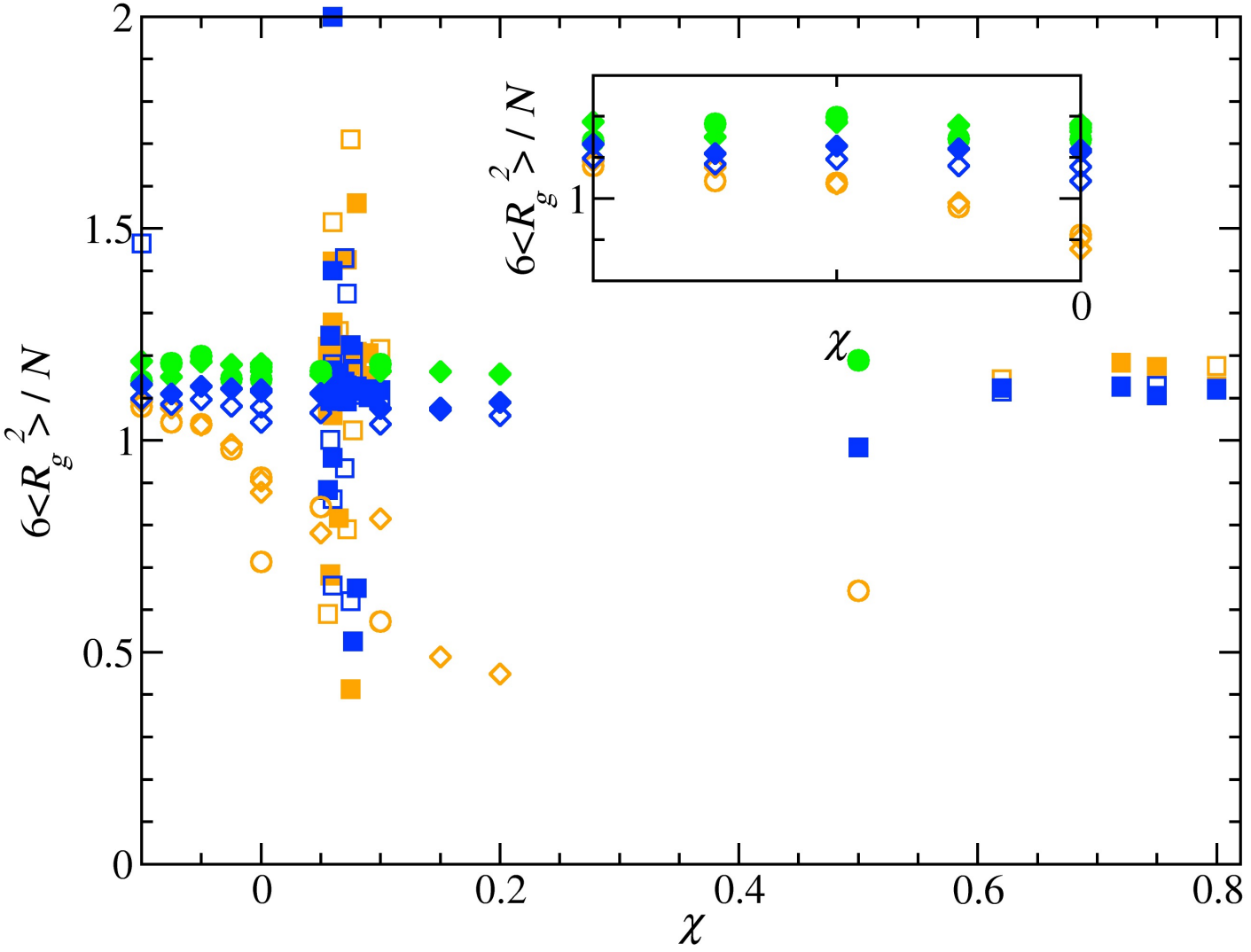

- SAN in SAN-dense (PMMA/SAN)
- SAN in SAN-dilute (PMMA/SAN)
- PMMA in SAN-dense (PMMA/SAN)
- PMMA in SAN-dilute (PMMA/SAN)
- SAN in SAN-dense (PGN $\phi_{\text{PMMA-m}}$=0.0)
- SAN in SAN-dilute (PGN $\phi_{\text{PMMA-m}}$=0.0)
- PMMA-g in SAN-dilute (PGN $\phi_{\text{PMMA-m}}$=0.0)
- SAN in SAN-dense (PGN $\phi_{\text{PMMA-m}}$=0.05)
- SAN in SAN-dilute (PGN $\phi_{\text{PMMA-m}}$=0.05)
- PMMA-g in SAN-dilute (PGN $\phi_{\text{PMMA-m}}$=0.05)
- PMMA-m in SAN-dense (PGN $\phi_{\text{PMMA-m}}$=0.05)
- PMMA-m in SAN-dilute (PGN $\phi_{\text{PMMA-m}}$=0.05)

- Grafts have a higher radius of gyration than the matrix in any phase
- Grafts are similar in binary and ternary mixtures
- PMMA matrix is longer in GNP phase
- SAN is longer in GNP phase
- Blend system gets weird near critical point (needs investigation)

Coarse-graining homopolymer blend system

Property	Experimental	TILD	CG MD
N_G	19 kDa	17	17
N_M	118 kDa	123	75
ρ_0		3.41	-
b		2.29 nm	1.53 nm (Kuhn length)
σ	0.7 chains/nm^2	3.69 chains/b^2 (0.27 chains/nm^2)	0.76 chains/d^2 (0.32 chains/nm^2)
R_{np}	7.5 nm	3.27 b (7.5 nm)	2.5 d (3.4 nm)

PMMA and SAN (33% Nitrile) ρ, b and χ from:

Aoki et al. Macromolecules, 52, 3, 1112-1124 (2019). 10.1021/acs.macromol.8b02431